

1 **A Single Trophoblast Layer Acts as the Gatekeeper at the Endothelial-Hematopoietic**
2 **Crossroad in the Placenta**

3 Pratik Home^{1,7@,*}, Ananya Ghosh^{1,8@}, Ram Parikshan Kumar^{1,2@,*}, Soma Ray¹, Sumedha
4 Gunewardena³, Rajnish Kumar¹, Purbasa Dasgupta¹, Namrata Roy¹, Abhik Saha¹, Madhu M.
5 Ouseph⁵, Gustavo W. Leone⁶, Soumen Paul^{1, 2, 4,*}

6 ¹Department of Pathology and Laboratory Medicine, ²Institute for Reproductive Health and
7 Perinatal Research, ³Department of Molecular and Integrative Physiology, ⁴Department of
8 Obstetrics and Gynecology, University of Kansas Medical Center, Kansas City, KS 66160,
9 USA. ⁵Department of Pathology and Laboratory Medicine, Weill Cornell Medical College, New
10 York, NY 10065. ⁶Department of Biochemistry, Medical College of Wisconsin, WI 53226, USA.
11 ⁷ Present address: XenoTech, A BioIVT Company, 1101 W Cambridge Cir Dr, Kansas City, KS
12 66103. ⁸ Present address: Department of Urology, University of California San Francisco, 35,
13 Medical 12 Center Way, San Francisco, CA 94143.

14 @ Equal contribution.

15 * Corresponding authors.

16 Correspondence: Soumen Paul (spaul2@kumc.edu), Pratik Home (phome@bioivt.com), Ram
17 Kumar (rkumar3@kumc.edu)

18

19 **Abstract**

20 During embryonic development the placental vasculature acts as a major hematopoietic niche,
21 where endothelial to hematopoietic transition ensures emergence of hematopoietic stem cells
22 (HSCs). However, the molecular mechanisms that regulate the placental hematoendothelial
23 niche are poorly understood. Using a parietal trophoblast giant cell (TGC)-specific knockout
24 mouse model and single-cell RNA-sequencing, we show that the paracrine factors secreted by
25 the TGCs are critical in the development of this niche. Disruptions in the TGC-specific
26 paracrine signaling leads to the loss of HSC population and the concomitant expansion of a
27 KDR+/DLL4+/PROM1+ hematoendothelial cell-population in the placenta. Combining single-
28 cell transcriptomics and receptor-ligand pair analyses, we also define the parietal TGC-
29 dependent paracrine signaling network and identify Integrin signaling as a fundamental
30 regulator of this process. Our study elucidates novel mechanisms by which non-autonomous
31 signaling from the primary parietal TGCs maintain the delicate placental hematopoietic-
32 angiogenic balance and ensures embryonic and extraembryonic development.

33

34 **Introduction**

35 Trophoblast cells of the placenta establish a vascular connection between the mother and the
36 fetus and express hormones that are essential for the successful progression of pregnancy.
37 Placenta also acts as one of the major organs for hematopoietic stem cell generation, and the
38 mid-gestation mouse placenta plays a significant role in the HSC development where it
39 provides a temporary niche for definitive HSC pool ¹⁻³. Defective development of placental
40 hematopoiesis and vasculogenesis leads to serious pathological conditions such as
41 preeclampsia and intra uterine growth restriction (IUGR)/ fetal growth restriction (FGR). These
42 disorders result in pregnancy-related complications, maternal, prenatal and neonatal mortality,
43 and affect ~2–8% of pregnant women worldwide ⁴. The pathogenesis in preeclamptic patients
44 is believed to be a response of vasculature to abnormal placentation ⁵. Thus, to define

45 therapeutic modalities against these pregnancy-associated disorders, it is crucial to
46 understand the molecular mechanisms that are associated with the proper development of
47 placental hematopoiesis and vasculogenesis.

48 Trophoblast cell differentiation in the placenta involves mechanisms by which secreted
49 paracrine factors within the placenta, and from the fetus and the mother regulate embryonic and
50 extraembryonic development ⁶. Embryonic hematopoietic sites are characterized by the
51 interlinked developments of the vascular and hematopoietic systems. Several studies have
52 shown that the hemangioblasts and hemogenic endothelium act as the presumptive precursors
53 to emerging hematopoietic cells ⁷. It has been indicated that the definitive hematopoiesis is
54 autonomously initiated in the placenta, which subsequently generates HSCs from hemogenic
55 endothelium and provides a niche for expansion of aorta-derived HSCs ^{3,8}. Moreover, secreted
56 pro-angiogenic factor, like Placental Growth Factor (PLGF), a member of the Vascular
57 Endothelial Growth Factor (VEGF) family, and anti-angiogenic factors, like soluble Vascular
58 Endothelial Growth Factor receptor-1 (sFLT1) and Endoglin (ENG), are expressed in the mouse
59 placenta, implying autocrine or paracrine actions ^{9,10}. How these signaling mechanisms
60 influence the development of the maternal-fetal interface are poorly understood.

61 Several studies have implicated GATA family of transcription factors in the development of
62 HSCs in other organs, and previously we have shown that GATA2 and GATA3 are involved in
63 the trophoblast development and differentiation ¹¹⁻¹⁵. They are implicated in the regulation of the
64 expression of several trophoblast-specific genes, including prolactin hormone Placental
65 lactogen I (*Pl3d1*, also known as *Pl1*) and the pro-angiogenic factor Proliferin (*Pl2c2*, also
66 known as *P1f*) ¹⁶⁻¹⁸. Recently we demonstrated that placenta-specific redundant functions
67 of *Gata2* and *Gata3* are important in trophoblast lineage development ¹⁹. The simultaneous
68 knockout of *Gata2* and *Gata3* resulted in significant developmental defects in the placenta as
69 well as the embryo proper, leading to very early embryonic lethality ¹⁹. These developmental
70 defects were accompanied by severe blood loss in the placenta, yolk sac, and the embryo

71 proper. Moreover, we established dual conditional *Gata2* and *Gata3* knockout trophoblast stem
72 cells and used ChIP-Seq and RNA-Seq analyses to define independent and shared global
73 targets of GATA2 and GATA3. We found that several pathways associated with the embryonic
74 hematopoiesis and angiogenesis are targets for both transcription factors¹⁹. However, very little
75 is known about how these two master regulators operate in a spatiotemporal manner within the
76 mature trophoblast during placental development and dictate placental hematopoiesis and
77 angiogenesis.

78
79 In a mouse conceptus, parietal trophoblast giant cells (parietal TGCs), which line the border of
80 the growing placenta and the maternal decidua, is thought to be a major source of endocrine
81 and paracrine signals during mouse placentation^{20,21}. Parietal TGCs are initially developed from
82 the trophoectoderm (primary parietal TGCs) and subsequently from the secondary
83 differentiation of precursors in the ectoplacental cone (secondary parietal TGCs). Gene
84 expression analyses revealed that both the primary and secondary parietal-TGCs specifically
85 express prolactin 3d1 gene (*Prl3d1*), also known as placental lactogen 1 (PL-1). Therefore, to
86 understand how GATA2/GATA3 functions could dictate endocrine and paracrine functions in a
87 developing placenta, we specifically deleted both *Gata2* and *Gata3* in the parietal TGC using
88 *Prl3d1^{tm1}(cre)Gle* (*PI1-Cre*) mouse line^{20,22,23} that drive Cre expression specifically within the
89 parietal TGCs. We noticed in-utero death of *Gata2/3* conditional double knockout
90 *Gata2^{ff};Gata3^{ff};PI1^{Cre/wt}* (GATA-PI1 KO) embryos starting from embryonic day 12.5 (e12.5). A
91 fraction of the GATA-PI1 KO embryos survived to birth. However, majority of the surviving
92 GATA-PI1 KO pups showed severe growth restriction. Remarkably, we noticed that along with
93 defect in trophoblast development, the delicate balance between hematopoietic vs angiogenic
94 differentiation is lost in the developing GATA-PI1 KO placentas. The GATA-PI1 KO placentas
95 showed severe defect in hematopoiesis due to reduced hematopoietic stem and progenitor cells
96 and disorganized placental vasculature due to defective differentiation of endothelial

97 progenitors. Thus, our study highlight the importance of a GATA-mediated transcriptional
98 program within a single trophoblast subtypes that fine-tunes the hematopoietic and endothelial
99 development during placentation.

100

101 **Results**

102 **GATA deletion in the trophoblast giant cell layer in mouse embryos display embryonic** 103 **and extraembryonic hematopoietic defects**

104 Our previous studies have shown that the loss of GATA factors in the trophoblast lineage cells
105 results in the gross phenotypic abnormality in the placenta and the embryo proper in a mouse
106 model ¹⁹. The placenta contains distinct layers of differentiated trophoblast cells, each having
107 specialized functions to support a pregnancy. These include TGCs, spongiotrophoblasts (SpT),
108 glycogen trophoblasts, and labyrinthine trophoblasts. Each subclass is characterized by their
109 unique gene expression signatures ²⁴. Thus, it is imperative to analyze how GATA factors act in
110 different subclasses of trophoblast cells in the context of placental development and function. As
111 TGCs have been reported to express both GATA2 and GATA3, we chose to delete *Gata2* and
112 *Gata3* together in the TGCs ¹⁶. Placental TGCs are marked by the expression of three prolactin
113 family of proteins Prl2c2 (PLF), Prl3b1 (PL2), Prl3d1 (PL1) and Cathepsin Q (CTSQ)²⁰. Out of
114 these four genes, PL1 expression is restricted to the parietal TGCs only . Thus, to restrict GATA
115 deletion exclusively to the parietal TGCs, we used a previously established *Prl3d1^{tm1(cre)Gle}*
116 (*Pl1^{Cre}*) mouse model ²², where Cre recombinase is selectively expressed in the *Pl1* expressing
117 cells (**Fig. S1A**). We validated the *Pl1*-specific Cre expression in this mouse model by LacZ
118 staining (**Fig. S1B**). We also developed a murine model in which the parietal trophoblast giant
119 cell layers were fluorescently labeled. We used *Gt(ROSA)26Sor^{tm4(ACTB-tdTomato,-EGFP)Lox/J}*, (also
120 known as *mT/mG*) mice, which possess loxP flanked membrane-targeted tdTomato (mT)
121 cassette and express strong red fluorescence in all tissues ²⁵. Upon breeding with the *Pl1*-Cre
122 recombinase expressing mice, the resulting offsprings have the mT cassette deleted in the Cre

123 expressing cells(s), allowing expression of the membrane-targeted EGFP (mG) cassette located
124 in-frame immediately downstream. Microscopic analyses of the conceptuses and their
125 cryosections from a cross between *PI1^{Cre}* male and *mT/mG* female confirmed the selective
126 EGFP fluorescence only in the parietal TGC layers (**Fig. S1C, Fig. 1A, B**). This expression of
127 *PI1-Cre* is consistent with the recent publication which clearly illuminates the PL1 protein
128 expression exclusively in the P-TGCs ²³.

129 Using *Gata2^{ff};Gata3^{ff}* mouse model reported in an earlier study from our laboratory, we
130 established a conditional GATA knockout mouse model *Gata2^{ff};Gata3^{ff};PI1^{Cre/wt}* (GATA-PI1 KO)
131 ¹⁹. Although a significant number of GATA-PI1 KO embryos showed lethality and abnormal
132 embryonic and extraembryonic phenotypes, a small percentage of them were viable. However,
133 almost all of them showed visible growth restriction at birth (**Fig. S2**). These viable growth
134 restricted pups were fertile and were chosen to function as breeders. For the embryo analyses,
135 we used these males for mating with non-Cre females to restrict the effect of GATA deletion
136 exclusively to the placental tissue. These mice were used to selectively knockout both *Gata2*
137 and *Gata3* in the parietal trophoblast giant cells. PCR with *Gata2* and *Gata3* deletion specific
138 primers confirmed the gene deletions specifically in the placenta in the GATA-PI1 KO and not in
139 the embryos (**Fig. S3A**). In addition, using laser captured microdissection (LCM) we excised
140 GFP-positive pTGCs from *Gata2^{ff};Gata3^{ff};PI1^{Cre/wt}* *mT/mG* placental sections. Again, PCR with
141 *Gata2* and *Gata3* deletion specific primers confirmed efficient deletion of the *Gata2* and *Gata3*
142 in these cells compared to the cells excised from adjacent labyrinth zone (**Fig. S3B**). Thus, we
143 validated that *Gata2* and *Gata3* could be efficiently deleted in a highly pTGC-specific manner in
144 the *Gata2^{ff};Gata3^{ff};PI1^{Cre/wt}* mouse model.

145 Previous studies have shown that the major expansion of the hematopoietic stem cell (HSC)
146 population in the mouse placenta takes place between E11.5 and E13.5 ¹. Thus
147 *Gata2^{ff};Gata3^{ff}; PI1^{Cre /wt}* males were crossed to *Gata2^{ff};Gata3^{ff}* females and the embryos were
148 analyzed between E10.5 and E13.5 (**Fig. 1C**). Resulting phenotypic abnormalities were

149 observed mostly at E12.5 and E13.5. For all subsequent analyses, E12.5 and E13.5
150 conceptuses were chosen.

151 Two major groups of embryos with distinct phenotypic abnormalities were observed in the *Pt1^{Cre}*
152 positive embryos (**Fig. 1D, E**). One group showed very early embryonic death and was
153 associated with extremely small fetal (necrotic) and placental tissues (**Fig. 1E, F**). The other
154 group showed significant growth restriction, developmental defects, and blood loss in the
155 embryo proper, while their placentae showed significant anomalies in size and weight and were
156 associated with apparent blood loss (**Fig. 1E, G, H**). These placentae showed apparent loss of
157 vasculature (**Fig. 1G**). These defects were most prominent at E12.5 and E13.5 (**Fig. S2**). Non-
158 Cre embryos from the same littermates were treated as controls (**Fig. 1E, G**). Along with these
159 gross abnormalities, significant alterations in the placental architecture were observed in the
160 GATA-PI1 KO samples. A marked increase in the junctional zone (marked by the
161 spongiotrophoblast/ glycogen trophoblast marker *Tpba*) was observed compared to the control
162 (**Fig. 1I-J**).

163 Interestingly, the fetal liver in the GATA-PI1 KO embryos showed blood loss (**Fig. 1G**), which is
164 consistent with the hypotheses that along with the hematopoietic stem and progenitor cells
165 (HSPCs) from the yolk sac, the placental HSCs migrate to and seeds fetal liver for
166 hematopoiesis²⁶.

167 Thus, our study showed that the GATA factor-loss in the parietal TGCs of the placenta was
168 sufficient to significantly impair embryonic and extraembryonic growth and also result in blood
169 loss and vasculature defects.

170

171 **GATA factor functions in parietal trophoblast giant cells regulate trophoblast progenitor** 172 **developments**

173 Some of the critical tasks of TGCs are the secretion of autocrine and paracrine factors that are
174 involved in the trophoblast outgrowth and placental development process^{27,28}. Genetic knockout

175 models targeting TGC specific genes have been shown to affect lineage-specific trophoblast
176 differentiation and thereby results in abnormal development of the placenta ^{22,27,29,30}. As mid-
177 gestation mouse placenta contains numerous cell types, including several different trophoblast
178 subtypes, endothelial cells, hematopoietic cells (both HSCs, multi-lineage cells, and terminally
179 differentiated cells), stromal cells, it is challenging to analyze the effect of a trophoblast-specific
180 gene knockout on placental cell subpopulations. To analyze the effect of GATA deletion in the
181 TGCs, we performed Single-cell RNA-Sequencing (scRNA-seq) analyses of E13.5 placenta
182 from a pregnant *Gata2^{ff};Gata3^{ff}* female crossed with *Gata2^{ff};Gata3^{ff}; Pl1^{Cre/wt}* male. Two
183 individual GATA-PI1 KO placentae and two individual control littermate placentae were used for
184 the sequencing. The genotypes were confirmed by PCR using tissue from the embryo
185 proper(genotype for GATA PI1-KO sample 1 is shown in **Fig. S3A**). The knockout placentae
186 where the apparent growth defects and blood loss phenotypes were most severe were chosen
187 for the scRNA-seq analysis (**Fig. 1G**).

188 T-distributed Stochastic Neighbor Embedding (t-SNE) plot of the aggregated hierarchical
189 clustering of the four samples revealed 33 distinct clusters (**Fig. 2A**). The clustering of both the
190 control samples showed significant similarity to each other, while significant clustering
191 similarities were observed in both the knockout samples, indicating a high degree of homology
192 between the placentae of the same genotypes (**Fig. S4**). To categorize the clusters, we
193 identified the top upregulated genes from each cluster (**Dataset 1**). Alongwith that, we used
194 "single-cell Mouse Cell Atlas (scMCA) analysis" pipeline previously described in a single-cell
195 RNAseq study on murine embryonic and extraembryonic tissues at E14.5 ³¹. We individually
196 fed digital gene expression (DGE) matrix for each cluster to scMCA which in turn used a
197 previously defined set of gene signatures ³¹ and predicted nature of that cluster with a
198 probability score. Alongwith that, it also listed top markers associated with that cluster. Finally,
199 we cross-matched the scMCA top markers from **Dataset 2** with the top markers we derived
200 earlier (**Dataset 1**). In this way we broadly identified five different cluster types in our samples.

201 They include trophoblast cells (clusters 1, 6, 7, 8, 9, 11, 16, 20, 21, 22, 24, 26, 33),
202 hematopoietic cells (cluster 2, 4, 5, 10, 12, 14, 17, 18, 28, 30, 31, 32), endothelial cells (clusters
203 15, 19, 29), endodermal cells (clusters 13, 27), and stromal cells (clusters 23, 25) (**Fig. 2B**,
204 **Dataset 2**). As scMCA could not predict the cell type for cluster 3, we looked at the top marker
205 expression for this cluster. It showed significant enrichment of several mitochondrial genes
206 (**Dataset 1**). Although contributions for the cluster 3 population came almost entirely from the
207 GATA PI1-KO samples (**Fig. 2C, S4**), the high level of mitochondrial gene enrichment in this
208 cluster implied dead cells captured during the library preparation for scRNA-seq. Thus Cluster 3
209 was excluded for subsequent analyses. However, we can not exclude the possibility of cluster 3
210 being a yet unknown. Aggregates of two control samples and GATA-PI1 KO placentae are used
211 and represented as Control and GATA-PI1 KO henceforth. Major alterations and rearrangement
212 of the trophoblast cell populations, which was associated with significant loss of the
213 hematopoietic cell populations, were evident in the GATA-PI1 KO placentae compared to the
214 control (**Fig. 2C**).

215 We also examined the enrichment of different trophoblast markers in individual trophoblast-
216 clusters based on their log₂-fold expression ratio of normalized mean gene UMI counts with a p-
217 value < 0.05 (**Dataset 2, 3**). Based on this analysis, we detected considerable gain in the
218 spongiotrophoblast population, including invasive spongiotrophoblasts, clusters 1, 7, 9, and 11,
219 which further validates our *in situ* hybridization observation above in **Fig. 1I-J (Fig. 2D)**. We also
220 observed a significant increase in the spiral artery-associated TGCs, clusters 8, 20, and 26 (**Fig.**
221 **2D**). This was accompanied by a significant loss in the high level of *Gjb3* expressing trophoblast
222 progenitor population, clusters 6 and 24 (**Fig. 2D**). Cluster 16, which showed strong expression
223 of syncytiotrophoblast markers *Dlx3*, *Tfeb*, *Hsd11b2*, gap junction protein *Gjb2*, PDGF receptor
224 α (*Pdgfra*), *Pparg*, *Slc16a1*, did not show significant changes in the GATA-PI1 KO placentae.

225 Although the scMCA analyses predicted cluster 33 to be of mixed nature including invasive
226 spongiotrophoblasts, spiral artery trophoblast giant cells and progenitor trophoblasts (**Dataset**

227 **2)**, we observed enrichment of several trophoblast giant cell associated genes in that cluster
228 (**Dataset 1**). They include pregnancy specific glycoproteins (*Psg23*, *Psg18*, *Psg19*,), several
229 prolactin family members (*Prl8a9*, *Prl7d1*, *Prl3b1*), Trophoblast-specific protein alpha (*Tpbpa*),
230 Endothelial protein C receptor (*Procr*), LIF receptor alpha (*Lifr*), Fibronectin 1 (*Fn1*). Moreover,
231 along with strong *Tpbpa* expression, cluster 33 also contained cells positive for *Prl3d1*, *Prl2c2*,
232 *Hand1*, *Prl3b1*, all markers for parietal trophoblast giant cells, spiral artery-associated
233 trophoblast giant cells, canal trophoblast giant cells, and sinusoidal trophoblast giant cells ³²
234 (**Fig. 2E**). Thus we identified cluster 33 as the TGC-cluster. Significantly, out of all the 33
235 clusters, only this cluster showed increased coexpression of *Prl3d1*, *Gata2* and *Gata3* (**Fig.**
236 **S5**). Interestingly, the loss of *Gata2* and *Gata3* in these cells did not seem to negatively affect
237 the parietal TGC population (**Fig. 2E, F**).

238 A comparison between the control sample and the knockout sample populations showed a
239 significant increase in the Trophoblast-specific protein alpha (*Tpbpa*) expressing cell population
240 (**Fig. 2E, F**). These cells were also found to be positive for Prolactin family member *Prl3b1*. On
241 the other hand labyrinth trophoblast progenitor cells marked by the expression of *Ly6a* (*Sca1*)
242 and high levels of Epcam (*Epcam*^{Hi}) ³³ and *Hand1* expressing cell population did not show any
243 significant alterations (**Fig. 2E, F**).

244 We also noticed defective syncytiotrophoblast (SynT) development in GATA-PI1 KO placentae.
245 The mouse labyrinth contains two layers of SynTs, namely SynT-I and SynT-II. which express
246 two distinct monocarboxylate transporters (MCTs). The SynT-I expresses MCT1 [also known as
247 Solute Carrier Family 16, Member 1 (SLC16A1)] and the SynT-II expresses MCT4 [also known
248 as Solute Carrier Family 16, Member 3 (SLC16A3)]. Recent studies revealed that the labyrinth
249 of a developing mouse placenta contains distinct progenitors for SynT-I and SynT-II layers^{15,23}.
250 The progenitors for SynT-I can be identified from the mRNA expression of *Glis1*, *Snap91*, *Stra6*,
251 *Tfrc*, *Epha4* and *Slc16a1*, whereas the progenitors of SynT-II can be identified from the mRNA
252 expression of *Igf1r*, *Egfr* and *Slc16a3*. From our scRNA-seq analyses, we noticed that the

253 relative abundance of The SynT-I progenitors were not altered in E12.5 GATA-PI1 KO
254 placentae (**Fig. S6A**). However, a significant increase in SynT-II progenitors was noticed in
255 GATA-PI1 KO placentae. We also noticed increased number of *Gcm1* expression is gradually
256 suppressed in SynTs after E9.5 and by E12.5 only a few SynT-II cells express *Gcm1* (**Fig.**
257 **S6B**). Thus, increased abundance of SynT-II precursors and *Gcm1* expressing cells indicate an
258 skewed SynT differentiation program in GATA-PI1 KO placentae. Together, these findings
259 revealed that the parietal TGC-specific loss of GATA factors skews the trophoblast
260 differentiation process and thereby alters the distribution of trophoblast subpopulations in the
261 developing placenta and affects gross placental architecture. Remarkably, these data also
262 indicate a novel mechanism whereby the parietal TGC-specific paracrine signaling dictates the
263 differentiation of the different trophoblast progenitors and regulates the development of distinct
264 placental layers.

265

266 **Loss of GATA factors disrupts hematopoietic-endothelial cell lineage segregation and** 267 **affects fetal hematopoiesis**

268 The placenta is one of the major sites for *de novo* hematopoiesis in an embryo ¹. It not only
269 supports the expansion of the nascent HSC population but also protects the HSCs from
270 premature differentiation cues. Several studies have implicated primary and secondary
271 trophoblast giant cells in secreting paracrine and endocrine factors ³⁴, which are thought to
272 regulate placental hematopoiesis. These include prolactin/ placental lactogen class of hormones
273 ³⁵, interferon ²⁸, vasodilators ³⁶, anticoagulants ³⁷ and several angiogenic factors ^{29,38,39}. In order
274 to analyze the effect of PL1-specific GATA factor loss on the placental hematopoietic cell
275 development, we used our scRNA-seq data. Ingenuity Pathway Analysis (IPA) was performed
276 to compare the physiological functions of the *Pri3d1*⁺ cells between the control and the KO
277 samples. Our results indicated that major physiological functions related to the hematopoiesis
278 and angiogenesis were downregulated in the *Pri3d1*⁺ cells in the GATA-PI1 KO samples (**Fig.**

279 **S7).**

280 We identified major hematopoietic subpopulations in our samples that include B-cells, T-cells,
281 Granulocytes, Macrophages, Erythroblasts, Dendritic cells, Basophils, Megakaryocytes,
282 Macrophages, and Natural Killer cells (**Fig. 3A, Dataset 2**). Placental HSCs are localized in the
283 labyrinth, and umbilical blood vessels⁴⁰ and have been shown to express surface markers KIT,
284 CD34, and Ly6A². We found two major clusters which harbored *Kit⁺ Cd34⁺ Ly6a⁺* cells, cluster
285 15 and cluster 17 (**Fig. 3A, B**). We calculated the relative percentages of cluster 15 and 17 cells
286 with respect to the total cell numbers per sample. While cells in the cluster 17 show gross
287 reduction in the GATA PI1-KO, cluster 15 displayed opposite trend. Almost all cells in cluster 15
288 were the contribution from the GATA PI1-KO placentae (**Fig. 3C**). Moreover, when we
289 calculated the relative percentages of the *Kit⁺ Cd34⁺ Ly6a⁺* HSC population, we found marked
290 reduction of these cells in the GATA PI1-KO compared to the control (**Fig. 3D**). Interestingly,
291 unlike 17, cluster 15 is marked by high level of expression of vascular endothelial growth factor
292 receptor- 2 (*Vgfr2/Kdr*) (**Fig. 3E**).

293 A hallmark of fetal hematopoiesis is the interrelated development of vascular and hematopoietic
294 systems where hemogenic endothelium and hemangioblasts serve as the precursors to the
295 hematopoietic stem cell populations⁴¹. Multiple studies have shown that the embryonic
296 hematopoiesis is intricately connected to the vascular development where hemogenic
297 endothelium, a part of the vascular endothelial cells, gives rise to the definitive hematopoietic
298 precursors during mammalian development⁴²⁻⁴⁴. Thus, the genetic signature of the cells in
299 cluster 15, which is unique to the knockout samples, indicates a hematoendothelial cell
300 population that still retains the HSC lineage markers. This cell population was also found to
301 express hematoendothelial markers *Cdh5*, *Icam2*, *Cd40*, confirming the bipotent nature of these
302 cells⁴⁵⁻⁴⁷ (**Fig. S8**). As a high expression of the arterial-specific marker *Delta-like, 4* (*Dll4*) is
303 essential for the segregation of the endothelial lineage from the hematopoietic lineage^{48,49}, we
304 looked at the *Dll4* expression in this subset, and found that this cluster expresses a high level of

305 *Dll4* (**Fig. 3E**). Curiously, cells in cluster 15 also showed expression of a recently identified
306 placental hemogenic endothelium marker *Prom1*^{50,51}, further confirming the hematoendothelial
307 nature of cluster 15 (**Fig. 3E-F**).

308 We further looked at the hematoendothelial population by further subjecting the placental cell
309 suspension to flow analysis. We screened single-cell suspension from control and GATA-PI1
310 KO placentae and filtered them against other hematopoietic lineage cells using antibody
311 specific for CD45, a pan-hematopoietic surface marker that appears on the more mature HSCs
312⁵², and a cocktail of hematopoietic lineage marker antibodies (Lin). These cells were further
313 screened for cells expressing CD34 and KDR simultaneously (**Fig. S9**). The percentage of this
314 hematoendothelial Lin⁻ CD45⁻ CD34⁺ KDR⁺ population showed significant increase in the GATA-
315 PI1 KO sample than the controls (**Fig. 3F, G**).

316 The result from the flow analysis mirrors the data from the scRNA-seq experiments (**Fig. 3C**)
317 and further confirms that the loss of GATA factors in the parietal TGCs skews the
318 hematopoietic-endothelial lineage specification in a developing placenta and leads to the arrest
319 of hematoendothelial progenitor population compared to the control.

320 In the next step, we used the three surface markers CD34, KIT (c-KIT), and Ly6A (SCA-1),
321 which together define the placental HSCs, as the determinant for the long-term reconstituting
322 (LTR) HSC population. Again, the cells were selected for CD45⁻ and Lin⁻ markers. These cells
323 were further subjected to flow analysis and were selected for KIT⁺ CD34⁺ Ly6A/E⁺ cells. In the
324 GATA-PI1 KO placental samples, the Lin⁻ CD45⁻ KIT⁺ CD34⁺ Ly6A/E⁺ cell population was
325 significantly reduced compared to the control (**Fig. 4A**). In comparison to the total number of
326 cells, the percentage of the HSC population in the KO placenta was significantly lower than that
327 in the control population (**Fig. 4B**) which resembles the results from the scRNA-seq analyses
328 (**Fig. 3D**).

329 Next, we evaluated the differentiation potential of the GATA-PI1 KO placental HSCs by using
330 the colony-forming assay. Placental single-cell suspension from the control and GATA-PI1 KO

331 placenta were plated on methylcellulose medium containing a cocktail of Stem Cell Factor
332 (SCF), IL-3, IL-6, and Erythropoietin. The placental samples gave rise to mostly granulocyte and
333 mixed lineage erythroid, macrophage colonies. We observed a significant reduction in the
334 number of colonies generated from the GATA-PI1 KO placenta compared to the control (**Fig.**
335 **4C, D**).

336 It is speculated that the placental HSCs migrate and seed fetal liver along with the HSCs (Lin-
337 Ly6A/E⁺ KIT⁺ (LSK)) from the aorta-gonad-mesonephros (AGM) ^{1,26,53,54}. In order to analyze the
338 fetal liver HSC population, we performed FACS analysis of the E13.5 fetal liver of the GATA
339 PI1-KO embryos and compared them to the control. We found significant depletion of the LSK
340 population in the GATA PI1-KO fetal livers compared to the controls (**Fig. S10**), which validated
341 our observation that the GATA PI1-KO embryos show blood loss in their fetal liver (**Fig. 1G**).

342 Collectively these data prove that the GATA factor KO in the trophoblast giant cells negatively
343 affects hematopoiesis in the placenta and fetal liver and results in the apparent blood loss
344 phenotype. The loss of the HSC population was also accompanied by the incomplete
345 segregation of the hematopoietic and endothelial lineage, indicating a loss of signaling network
346 that balances and fine-tunes the hematopoietic versus endothelial cell lineage development in
347 the placenta.

348

349 **TGC-specific loss of GATA factors affects placental vasculature development**

350 Embryonic hematopoiesis and angiogenesis are tightly linked. Hemogenic endothelium in the
351 vascular labyrinth gives rise to both the endothelial cell population as well as the hematopoietic
352 cell population. As our study revealed a defective hematopoietic and endothelial lineage
353 segregation due to TGC-specific GATA factor loss, we used our GATA-PI1 KO placenta model
354 to test placental angiogenesis. Anti-CD31 (PECAM-1) antibody, which marks early and mature
355 endothelial cells, was used to stain the vasculature in the placental sections at E13.5.
356 Compared to the control samples, the KO placenta showed gross disruption of the blood

357 vessel architecture in the labyrinth (**Fig. 5A, B**)

358 Embryonic angiogenesis relies on a delicate balance of several key pro-angiogenic and anti-
359 angiogenic factors^{55,56}. Among them anti-angiogenic factor soluble Vascular Endothelial Growth
360 Factor (VEGF) receptor FLT1 (sFLT1) has been shown to play essential roles in the placental
361 vascularization and angiogenesis^{57,58}. Our results showed upregulation of *Flt1* in the GATA-PI1
362 KO placentae compared to the control (**Fig. 5C**). The sc-RNAseq data also showed that the
363 highest upregulation of *Flt1* in the GATA PI1-KO placentae was associated with cluster 33,
364 previously identified in this study as the TGC cluster (**Fig. 5D, E**). Other prominent sources of
365 Flt1 expression were the hematoendothelial cells (cluster 15), spongiotrophoblast cells in
366 clusters 1, 9, 11, and spiral artery associated TGCs in cluster 26 (**Fig. 5D**).

367 To functionally test the increase in the *Flt1* level, we performed matrigel based vascular tube
368 formation assays using Human Uterine Microvascular Endothelial Cells (HUtMEC). As
369 differentiated trophoblast stem cells express antiangiogenic sFLT1, we harvested conditioned
370 media from the differentiated *Gata2/Gata3* double knockout (GATA DKO) trophoblast stem cells
371 and differentiated control trophoblast stem cells described in our earlier study¹⁹. These
372 conditioned media were added to the assays individually. Interestingly, HUtMECs in the
373 presence of the conditioned media from the control trophoblast stem cells readily formed tubular
374 structure while they failed to do so in the presence of conditioned media from GATA DKO
375 trophoblast stem cells (**Fig. 5F**).

376 These findings indicate that the loss of GATA factors in the TGC layer results in the disruption of
377 the delicate balance between the secreted angiogenic and anti-angiogenic factors by direct
378 upregulation of *Flt1* expression in the TGC cells and by increasing the numbers of *Flt1*
379 expressing trophoblast cells. This overall rise in the FLT1 level, in turn prevents proper
380 development of the labyrinth vasculature in the placenta.

381

382 **GATA loss alters trophoblast giant cell-mediated paracrine signaling**

383 TGCs are known to be a major source of autocrine and paracrine factors in the placenta ^{32,59}.
384 These factors, in turn, influence the development of the placenta as well as regulate numerous
385 placental functions. In order to analyze the TGC-mediated signaling mechanism that regulates
386 the development of placental trophoblast subpopulations and dictate hematoendothelial
387 differentiation, we employed a recently reported bioinformatic tool PyMINER ⁶⁰. PyMINER
388 identifies receptor-receptor and ligand-receptor pairs by filtering out cell type-enriched receptors
389 or secreted ligand genes. It then builds up a network of protein level interactions within and
390 across all cell types by cross-referencing gene-gene pairs for physical protein-protein
391 interactions. Finally, PyMINER uses pathway analyses to identify the autocrine or paracrine
392 signaling mechanism for these cell types. We used all the 33 clusters as input to PyMINER to
393 ensure correlation with the rest of our analyses. We identified several cross-cluster ligand-
394 receptor pairs across our identified clusters. As we were interested in the paracrine signaling
395 emanating from *Pr13d1+* cluster 33, we evaluated all extracellular ligand pairs for corresponding
396 receptor matches in other clusters. PyMINER analysis indicated the HSCs and HSPCs (cluster
397 17), and the hematoendothelial population (cluster 15), among the major paracrine signaling
398 targets for extracellular factors expressed by the *Pr13d1+* cluster 33 (**Fig. 6A**). This analysis also
399 suggested laminin subunits *Lamb1*, *Lamb2*, *Lamc3*, *Lama5*, Collagen type IV alpha 1 (*Col4a1*),
400 Fibronectin 1 (*Fn1*), and *Ccl27a* as possible major paracrine regulators acting on cluster 17
401 (**Dataset 4**). Similarly, our data suggested *Lamb1*, *Lamb2*, *Lamc3*, *Lama5*, Collagen type IV
402 alpha 1 (*Col4a1*), Fibronectin 1 (*Fn1*), Lymphocyte antigen 96 (*Ly96*) and *Wnt11* to be the major
403 potential paracrine factors acting on the hematoendothelial cluster 15 (**Fig. 6A**). When these
404 genes were subjected to PANTHER pathway analysis, we observed significant enrichment of
405 the Integrin signaling pathway in both the cases (**Fig. S11A**). The integrin signaling pathway has
406 been implicated in both mouse and human placental development ⁶¹.
407 Interestingly, it has been shown that knocking out Integrin Subunit Alpha 5 (*Itga5*) in mice
408 results in embryonic lethality for a large number of the embryos and shows poor development of

409 the placental labyrinth and poor interdigitation of fetal and maternal vessels⁶². Also, knocking
410 out Integrin Subunit Alpha 7 (*Itga7*) in mice results in defective placental structures, including
411 infiltration of the spongiotrophoblast layer into the placental labyrinth⁶³.

412 Moreover, our data pointed to two trophoblast clusters, progenitor trophoblasts (cluster 6), and
413 labyrinthine trophoblasts (cluster 16) as the potential targets for 28 paracrine factors expressed
414 by cluster 33 (**Fig. 6A**). These groups of paracrine factors included the Integrin signaling
415 pathway members identified above, along with 16 prolactin family of hormones and Inhibin beta
416 B (*Inhbb*) (**Dataset 4**). While the Prolactin family of genes has been studied extensively in the
417 context of placental development and function^{64,65}, *Inhbb* has been implicated in preeclampsia
418⁶⁶.

419 We analyzed these genes for GATA factor occupancy using our previously published data¹⁹.
420 Interestingly, we found about half of these genes (*Col4a1*, *Col4a2*, *, *Inhbb*, *Lama5*, *Lamb1*,
421 *Lamb2*, *Lamc3*, *Ly96*, *Prl2a1*, *Prl7d1*, *Wnt11*) to be putative GATA targets (**Fig. S11B-C**).
422 Further analysis with the *Prl3d1*-positive cells in the cluster 33 showed upregulation of *Col4a1*,
423 *Col4a2*, *Fn1*, *Inhbb*, *Lama5*, *Lamb1*, *Lamb2*, *Lamc3*, while downregulation of *Prl2a1*, *Prl2c2*,
424 *Prl2c5*, *Prl4a1*, *Prl7d1* (**Fig. 6B**).*

425 Among the suggested paracrine factors associated with the pTGCs in the GATA PI1-KO
426 placentae, we tested the expression level of LAMB1 and LAMB2. Immunostaining revealed
427 increased expression levels of these two factors in the KO samples compared to the controls
428 (**Fig. 6C**).

429 Collectively, these results suggest that inhibition of the Integrin signaling pathway in the parietal
430 TGCs might be critical for hematoendothelial differentiation and maintaining hematopoietic-
431 angiogenic balance in the developing mouse placenta. Our data also indicated that repression
432 of the integrin signaling pathway along with the activation of the prolactin signaling might play a
433 crucial part in the trophoblast lineage differentiation and helps maintain the proper ratio of
434 placental trophoblast subtypes (**Fig. 7**).

435

436 **Discussion**

437 GATA factor function in trophoblast differentiation and function has been subjected to numerous
438 studies. Previously, we showed how GATA2 and GATA3 have overlapping functions during
439 placental development, where the simultaneous loss of both the factors in all trophoblast cells
440 leads to early embryonic death and placental defect with impaired hematopoiesis^{14,19}. It also
441 revealed the loss of placenta layers, including the labyrinth region. Interestingly, the pan-
442 trophoblast-specific knockout did not show significant change in the trophoblast giant cell
443 numbers at the junctional zone.

444 As the placenta is a complex tissue consisting of diverse trophoblast subtypes as well as
445 hematopoietic and endothelial cell populations, it is of utmost importance to categorize these
446 cellular subtypes and define cell-cell interactions at the single-cell resolution. A recent study in
447 mouse placenta employed single-nuclei RNAseq to highlight labyrinth development, but left out
448 the role of the parietal TGCs⁶⁷. Although due to the inherent technical limitations of the 10X
449 genomics sc-RNAseq platform we could only capture a small fraction of the
450 syncytiotrophoblasts and TGCs, our analyses successfully identified the TGC cluster and the
451 syncytial layers. Our sc-RNASeq data not only predicted the genetic signatures of the major
452 trophoblast subtypes but also showed how the pTGC-specific transcriptional program governs
453 the differentiation of the progenitor population and thereby altered the distribution of cells at
454 different placental layers. Data from our *Gata2^{ff};Gata3^{ff};Pl1^{Cre/wt}* mouse models showed that the
455 loss of the GATA factors in the parietal TGC population severely reduced the placental size and
456 also led to fetal growth restriction with significant phenotypic abnormality between E12.5 and
457 E13.5. Importantly, we observed significant structural changes in the GATA-PI1 KO placentae
458 compared to the control. Molecular and morphological analyses revealed gross redistribution of
459 different trophoblast progenitor cells, including *Prl2c2* expressing giant cells, *Tpbpa* expressing
460 spongiotrophoblast progenitor, *Prl3b1* expressing secondary giant cell progenitors. While the

461 number of *Epcam* expressing labyrinth progenitor cells showed a marked increase, we did not
462 observe any significant enlargement of the labyrinth regions in the GATA-PI1 KO placentae
463 when normalized against the total placental area. In total, these findings reveal how different
464 layers of trophoblast cells interact during placental development and influence the differentiation
465 of trophoblast progenitors.

466 TGCs in the placenta secrete a lot of cytokines and hormones, which are not only crucial for
467 trophoblast differentiation and placental development but are also critical for placental
468 angiogenesis and hematopoiesis. Our study predicted possible mechanisms through which
469 TGC-specific GATA factors dictate TGC-specific paracrine signaling and, in turn, regulate
470 placental hematoendothelial niche. Curiously, the loss of TGC-specific GATA factors resulted in
471 a unique cell population marked by the expression of *Kdr*, as well as *Kit*, *Cd34*, and *Ly6A*. The
472 expression of both the endothelial gene and hematopoietic stem cell markers indicated towards
473 the emergence of a hematoendothelial cell cluster. The complete absence of this cell population
474 in the control placentae also indicated differentiation of these cells in the absence of TGC-
475 specific GATA factors.

476 The GATA-PI1 KO placentae were further characterized by the lack of proper angiogenic
477 reorganization in the labyrinth. Our observation about the increased level of *Flt1* gives us a
478 possible explanation about the angiogenic defect. The concomitant expansion of the *Tpbpa*
479 expressing spongiotrophoblast in the GATA-PI1 KO could also contribute to the impairment of
480 the labyrinth development. We speculate that this loss in the surface area of exchange may
481 result in the reduction of the nutrient supply and finally result in fetal growth restriction.

482 The integrin signaling pathway has been extensively studied in relation to the placental
483 development as well as angiogenesis in both rodents and humans. Our novel finding suggests
484 potential mechanisms by which inhibition of the integrin signaling pathway promotes placental
485 hematoendothelial differentiation. This brings a new insight into how a small number of parietal
486 trophoblast giant cells at the maternal-fetal interface can dictate the hematopoietic and

487 angiogenic development in the placenta and thereby can affect fetal development.

488 Mouse embryogenesis involves vascularization on both the placental side as well as the
489 decidual side. TGCs secrete a lot of angiogenic and anti-angiogenic paracrine factors, and in
490 turn, regulate the decidual vascularization. However, how these factors dictate decidual
491 vascularization, is poorly understood. It would be interesting to study how TGC-specific loss of
492 GATA factors affect decidualization and associated vascular development. In this aspect, our
493 TGC-specific GATA knockout mouse model holds great promise to help investigate the
494 paracrine signaling from the TGC layers involved in the decidual angiogenesis.

495 GATA2 and GATA3 are evolutionarily conserved among mammals, and they are expressed in
496 the human placenta. However, unlike the mouse placenta, human placental layers do not have
497 trophoblast giant cells. In the absence of defined TGC subtypes, it is impossible to analyze the
498 role of GATA factors in the placental development in humans. Moreover, ethical and logistical
499 issues make it impossible to examine the role of GATA factors in human placental development
500 *in vivo*. Nonetheless, the recent establishment of a human trophoblast cell line ⁶⁸ has presented
501 us with a new tool to examine the role of GATA factors in human placental development. As
502 these cells can be readily differentiated *in vitro* to extravillous trophoblast and
503 syncytiotrophoblast subtypes, they open the possibility of serving as models to study the role of
504 GATA factors in the context of human placental development.

505 GATA2 and GATA3 are evolutionarily conserved among mammals, and they are expressed in
506 the human placenta^{19,69}. Although a human placenta does not have a Junctional zone, the TGC
507 population resembles with the extravillous trophoblast cells (EVTs) of a human placenta. EVT
508 arise at the anchoring villi (which anchor the placenta with the uterine tissue) within a
509 developing human placenta and invades into the uterine compartment⁶⁹. A subset of EVT
510 population migrates deeply into the uterus and upto the first third of the myometrium, where they
511 differentiate to a giant cell population ^{70,71}, which undergo endoreduplication, similar to the
512 mouse parietal TGCs. These human invasive EVT-derived giant cells also mediate paracrine

513 signaling to modulate the uterine microenvironment⁷¹. Intriguingly both GATA2 and GATA3 are
514 highly expressed in invasive EVT_s at the human maternal-fetal interface. Thus, it will be
515 interesting to find out how GATA2 and GATA3 regulate gene expression dynamics in human
516 EVT_s. Successful establishment of bona-fide human trophoblast stem cell lines⁶⁸ has
517 presented us with a new tool to examine this aspect and opens up the possibility of serving as
518 models to better understand the role of GATA factors in the context of human placental
519 development.

520 **Materials and methods**

521 **Generation of conditional knockout mice strains**

522 All procedures were performed after obtaining IACUC approvals at the Univ. of Kansas Medical
523 Center. Female *Gata2*^{flox/flox} (*Gata2*^{ff}) mice⁷² were mated with *Pr13d1tm1(cre)Gle* (*PI1*^{Cre})
524 male in order to generate *Gata2*^{ff/+}; *PI1*^{Cre/wt}. In the next step, *Gata2*^{ff/+}; *PI1*^{Cre/wt} female mice were
525 bred with *Gata2*^{ff/+}; *PI1*^{Cre/wt} males to generate *Gata2*^{ff/ff}; *PI1*^{Cre/wt}. Similarly female *Gata3*^{flox/flox}
526 (*Gata3*^{ff}) mice⁷³ were used to generate *Gata3*^{ff/ff}; *PI1*^{Cre/wt}. In the next step, *Gata2*^{ff/ff}; *PI1*^{Cre/wt} and
527 *Gata3*^{ff/ff}; *PI1*^{Cre/wt} mice were crossed to generate *Gata2*^{ff/+}; *Gata3*^{ff/+}; *PI1*^{Cre/wt}. Later
528 *Gata2*^{ff/+}; *Gata3*^{ff/+}; *PI1*^{Cre/wt} males and females were crossed to generate *Gata2*^{ff/ff}; *Gata3*^{ff/ff}; *PI1*^{Cre/wt}
529 strain. Further crosses with Gt(ROSA)26Sortm4(ACTB-tdTomato,-EGFP)Luo/J, (also known as
530 mT/mG) mouse strain was used to establish *Gata2*^{ff/ff}; *Gata3*^{ff/ff}; *mT/mG* mouse line.

531 **Embryo harvest and tissue isolation**

532 Animals were euthanized on desired day points, as indicated in the main text. Uterine horns and
533 conceptuses were photographed. Conceptuses were dissected to isolate embryos, yolk sacs,
534 and placentae. All embryos and placentae were photographed at equal magnification for
535 comparison purposes.

536 Uteri containing placentation sites were dissected from pregnant female mice on E12.5 and
537 E13.5 and frozen in dry ice-cooled heptane and stored at -80°C until used for histological
538 analysis. Tissues were subsequently embedded in optimum cutting temperature (OCT) (Tissue-

539 Tek) and were cryosectioned (10 μ m thick) for immunohistochemistry (IHC) studies using Leica
540 CM-3050-S cryostat.

541 Placenta samples were carefully isolated, ensuring the decidual layer was peeled off. Individual
542 samples were briefly digested in the presence of collagenase and were made into single-cell
543 suspensions by passing them through a 40 μ m filter. These cell suspensions were further used
544 for Flow analysis or FACS. Corresponding embryonic tissues were used to confirm genotypes.

545 For scRNA-seq, these samples were further processed using Debris Removal Solution and
546 Dead Cell Removal Kit (Miltenyi Biotec). Red blood cell depletion from the placental
547 suspensions were carried out using anti-Mouse Ter-119 antibody (BD Biosciences) was used.

548 **Single Cell RNA-Sequencing and analysis**

549 The transcriptomic profiles of mouse placental samples from two control (biological replicates)
550 and two *Gata2/Gata3* double knockout (biological replicate) specimens were obtained using the
551 10x Genomics Chromium Single Cell Gene Expression Solution (10xgenomics.com). The
552 primary analysis of the scRNA-seq data was performed using the 10x Genomics Cell Ranger
553 pipeline (version 3.1.0). This pipeline performs sample de-multiplexing, barcode processing, and
554 single-cell 3' gene counting. The quality of the sequenced data was assessed using the FastQC
555 software ⁷⁴. Sequenced reads were mapped to the mouse reference genome (mm10) using the
556 STAR software ⁷⁵. Individual samples were aggregated using the “cellranger aggr” tool in Cell
557 Ranger to produce a single feature-barcode matrix containing all the sample data. This process
558 normalizes read counts from each sample, by subsampling, to have the same effective
559 sequencing depth. The Cell Ranger software was used to perform two-dimensional PCA and t-
560 SNE projections of cells, and k-means clustering. The 10x Genomics Loupe Cell Browser
561 software (v 4.1.0) was used to find significant genes, cell types, and substructure within the
562 single-cell data.

563 Digital Gene Expression matrices for each clusters identified using Cell Ranger, were
564 individually fed into the scMCA pipeline (<http://bis.zju.edu.cn/MCA/blast.html>). scMCA output
565 consisted of top markers for each clusters, predicted probabilities for the clusters alongwith their
566 *p*-values. Clusters were identified using the smallest *p*-value. Where multiple equal probabilities
567 existed, we calculated the abundance of the top markers in the respective clusters and also
568 looked at the rest of the genes expressed in that cluster to attribute cell types in that cluster.
569 Using Ingenuity Pathway Analysis (Qiagen) software, we performed a core analysis of the
570 significantly ($p \leq 0.05$) upregulated transcripts in the *Pr3d1+* cell clusters from the control and
571 the GATA PI1-KO scRNA-seq transcriptomes. The core analyses results were then compared
572 and filtered for physiological functions related to hematopoiesis and angiogenesis to generate
573 the heatmap.

574 PyMINER analysis was performed using methods described by Tyler *et al.*⁶⁰. Clusters defined
575 by the Cell Ranger were used as input. The receptor-ligand pairs were sorted on a PyMINER
576 score. Pairs with a score more than 800 were retained to introduce high stringency. PANTHER
577 pathway analysis was done using the predicted paracrine secreted ligands from cluster 33.
578 Corresponding gene list were supplied as input.

579 **Cell culture and reagents**

580 Mouse trophoblast stem cells (TSCs) were cultured with FGF4, Heparin, and MEF-conditioned
581 medium (CM) according to protocol⁷⁶. *Gata2* and *Gata3* floxed alleles were efficiently excised
582 from *Gata2^{ff};Gata3^{ff};UBC-cre/ERT2* (GATA DKO) TSCs by culturing the cells in absence of
583 FGF4 and MEF-conditioned media and in the presence of tamoxifen (1 μ g/ml)¹⁹. Conditioned
584 media was harvested upon removal of tamoxifen and was used for subsequent experiments.

585 **Flow analysis and sorting**

586 For analyzing HSC population, placental single-cell suspensions were stained with APC-
587 conjugated anti-mouse CD117 (c-Kit) (BioLegend), PerCP/Cy5.5-conjugated anti-mouse CD34
588 (BioLegend), PE-conjugated anti-mouse Ly-6A/E (Sca-1) (BioLegend), PE/Cy7 anti-mouse

589 CD45 (BioLegend) and Pacific Blue-conjugated anti-mouse Lineage cocktail (BioLegend)
590 monoclonal antibodies. Unstained, isotype and single-color controls were used for optimal
591 gating strategy. Samples were run on either an LSRII flow cytometer or an LSRFortessa (BD
592 Biosciences), and the data were analyzed using FACSDiva software.

593 Similarly, E13.5 fetal liver cells were also stained with APC-conjugated anti-mouse CD117 (c-
594 Kit) (BioLegend), PE-conjugated anti-mouse Ly-6A/E (SCA-1) (BioLegend), and Pacific Blue-
595 conjugated anti-mouse Lineage cocktail (BioLegend) monoclonal antibodies.

596 **Colony Formation Assay**

597 Placenta cell suspensions were suspended in Iscove's MDM with 2% fetal bovine serum and
598 cultured using a MethoCult GF M3434 Optimum kit (STEMCELL Technologies). 10,000 cells
599 from each sample were plated in 35-mm culture dishes (STEMCELL Technologies) and
600 incubated at 37°C in a humidified, 5% CO₂ environment for 14 days. Colonies were observed
601 and counted using an inverted microscope.

602 ***In-Vitro* Endothelial Network Assembly Assay on Matrigel**

603 Endothelial network assembly was assayed by the formation of capillary-like structures by
604 HUtMECs on Matrigel (BD Biosciences). Matrigel was diluted 1:1 with a supplement-free M200
605 medium, poured in 12-well plates, and allowed to solidify at 37 °C. Sub confluent HUtMECs
606 were harvested and preincubated for 1 hour in growth supplement-free M200 medium in
607 microcentrifuge tubes. An equal volume of M200 medium containing FGF2/EGF was added. In
608 addition, conditioned medium from differentiated *Gata2^{ff};Gata3^{ff};UBC^{CreERT2}* trophoblast stem
609 cells cultured in the presence (control) and absence of tamoxifen (GATA DKO) were added. The
610 cells were plated on Matrigel (1.5 × 10⁵ cells/well) and incubated at 37 °C and photographed at
611 different time intervals.

612 **Quantitative RT-PCR**

613 Total RNA from cells was extracted with the RNeasy Mini Kit (Qiagen). Samples isolated using
614 FACS were further processed using the PicoPure RNA Isolation kit. cDNA samples were
615 prepared and analyzed by qRT-PCR following procedures described earlier ¹⁴.

616 **Genotyping**

617 Genomic DNA samples were prepared using tail tissues or embryonic tissues from the mice
618 using the REExtract-N-Amp Tissue PCR kit (Sigma-Aldrich). Genotyping was done using
619 REExtract-N-Amp PCR ReadyMix (Sigma-Aldrich) and respective primers. Respective primers
620 are listed in the materials and methods section.

621 **Immunofluorescence**

622 For immunostaining with mouse tissues, slides containing cryosections were dried, fixed with
623 4% PFA followed by permeabilization with 0.25% Triton X-100 and blocking with 10% fetal
624 bovine serum and 0.1% Triton X-100 in PBS. Sections were incubated with primary antibodies
625 overnight at 4 °C, washed in 0.1% Triton X-100 in PBS. After incubation (1:400, one hour, room
626 temperature) with conjugated secondary antibodies, sections were washed, mounted using an
627 anti-fade mounting medium (Thermo Fisher Scientific) containing DAPI and visualized using
628 Nikon Eclipse 80i fluorescent microscope.

629 *mT/mG* positive embryos and cryosections were imaged directly under a Nikon Eclipse 80i
630 fluorescent microscope.

631 **In situ hybridization**

632 E13.5 whole conceptus cryosections were subjected to staining using RNAscope 2.5 HD
633 Detection Kit (ACD Bio, Newark, CA). RNAscope probe for *Tpbpa* was used to detect the
634 junctional zone of the mouse placenta, while hematoxylin was used as the counterstain.

635 **Statistical analyses**

636 Independent data sets were analyzed using GraphPad Prism software. Two-tailed Student's t-
637 tests were performed for significance and the data are presented as mean±s.e.m.

638

639 **Primer List**

640 **Primers used for genotyping**

Gata2- floxed and Gata2- null	GCCTGCGTCCTCCAACACCTCTAA	TCCGTGGGACCTGTTTCCTTAC
Gata3- flox	CAGTCTCTGGTATTGATCTGCTTCTT	GTGCAGCAGAGCAGGAAACTCTCAC
Gata3- null	TCAGGGCACTAAGGGTTGTAACTT	GTGCAGCAGAGCAGGAAACTCTCAC
Cre	AAAATTTGCCTGCATTACCG	ATTCTCCCACCGTCAGTACG

641

642 **Antibody list**

643 **Immunostaining**

Primary antibodies	Species raised in	Vendor	Catalog number	Dilutions used
anti-mouse CD31	Rat	BD Pharmingen	553369	1:100
anti-Laminin beta 1 [LT3]	Rat	Abcam	ab44941	1:100
Anti-Laminin beta 2	Mouse	Developmental Studies Hybridoma Bank	C4	1:1
Secondary antibodies	Species raised in	Vendor	Catalog number	Dilutions used
Alexa Fluor 488 anti-mouse	Donkey	Abcam	ab150105	1:400

IgG				
Alexa Fluor 568 anti-rat IgG	Donkey	Abcam	ab175475	1:400
Antibodies used in FACS	Species raised in	Vendor	Catalog number	
APC anti-mouse CD117 (c-kit)	Rat	BioLegend	105812	
PerCP/Cy5.5 anti-mouse CD34	American Hamster	BioLegend	128607	
PE anti-mouse Ly-6A/E (Sca-1)	Rat	BioLegend	108108	
PE/Cy7 anti-mouse CD45	Rat	BioLegend	103113	
Pacific Blue anti-mouse Lineage Cocktail	Rat	BioLegend	133310	
Alexa Fluor 488 anti-mouse CD309 (VEGFR2, Flk-1)	Rat	BioLegend	121908	

644

645 **Data availability**

646 Processed data can be accessed from the NCBI Gene Expression Omnibus database
 647 (accession number GSE163286).

648 **Acknowledgment**

649 This study is supported by various core facilities, including the Genomics Core, the Imaging and
650 Histology Core facility, and the Bioinformatics Core of the University of Kansas Medical Center.

651

652 **Conflict of interest**

653 The authors declare no competing interests.

654

655 **Funding**

656 This research was supported by NIH grants HD062546, HD0098880, HD079363, and a bridging
657 grant support under the Kansas Idea Network of Biomedical Research Excellence (K-INBRE,
658 P20GM103418) to SP. A pilot grant under NIH Center of Biomedical Research Program
659 (COBRE, P30GM122731) supported to PH. This study was also supported by various core
660 facilities, including the Genomics Core, Imaging and histology Core facility, and the
661 Bioinformatics Core of the University of Kansas Medical Center.

662

663 **Data availability**

664 All the sequencing data are available and will be uploaded in a public database upon
665 acceptance of this manuscript.

666

667 **Contribution**

668 R.P.K. and S.P. conceived, designed and performed the initial study. P.H., RPK and A. Ghosh,
669 performed the main experiments. P.H., A. Ghosh., R.P.K., and S.R. analyzed data. S.G., P.H.
670 and R. K analyzed genomics data. P.H. wrote the manuscript. PH and RPK Revised the
671 manuscript. S.P. edited the final manuscript.

672 References

- 673 1. Gekas, C., Rhodes, K.E., Van Handel, B., Chhabra, A., Ueno, M., and Mikkola, H.K.
674 (2010). Hematopoietic stem cell development in the placenta. *Int J Dev Biol* *54*, 1089-
675 1098. [10.1387/ijdb.103070cg](https://doi.org/10.1387/ijdb.103070cg).
- 676 2. Ottersbach, K., and Dzierzak, E. (2005). The murine placenta contains hematopoietic
677 stem cells within the vascular labyrinth region. *Developmental Cell* *8*, 377-387. DOI
678 [10.1016/j.devcel.2005.02.001](https://doi.org/10.1016/j.devcel.2005.02.001).
- 679 3. Rhodes, K.E., Gekas, C., Wang, Y., Lux, C.T., Francis, C.S., Chan, D.N., Conway, S.,
680 Orkin, S.H., Yoder, M.C., and Mikkola, H.K. (2008). The emergence of hematopoietic
681 stem cells is initiated in the placental vasculature in the absence of circulation. *Cell Stem*
682 *Cell* *2*, 252-263. [10.1016/j.stem.2008.01.001](https://doi.org/10.1016/j.stem.2008.01.001).
- 683 4. Duley, L. (2009). The global impact of pre-eclampsia and eclampsia. *Seminars in*
684 *perinatology* *33*, 130-137. [10.1053/j.semperi.2009.02.010](https://doi.org/10.1053/j.semperi.2009.02.010).
- 685 5. Lindheimer, M.D., Roberts, J.M., Cunningham, F.G., and Chesley, L.C. (2009).
686 Chesley's hypertensive disorders in pregnancy, 3rd Edition (Academic Press/Elsevier).
- 687 6. Iliodromiti, Z., Antonakopoulos, N., Sifakis, S., Tsikouras, P., Daniilidis, A., Dafopoulos,
688 K., Botsis, D., and Vrachnis, N. (2012). Endocrine, paracrine, and autocrine placental
689 mediators in labor. *Hormones (Athens)* *11*, 397-409.
- 690 7. Nishikawa, S.I. (2001). A complex linkage in the developmental pathway of endothelial
691 and hematopoietic cells. *Curr Opin Cell Biol* *13*, 673-678.
- 692 8. Koushik, S.V., Wang, J., Rogers, R., Moskophidis, D., Lambert, N.A., Creazzo, T.L., and
693 Conway, S.J. (2001). Targeted inactivation of the sodium-calcium exchanger (Ncx1)
694 results in the lack of a heartbeat and abnormal myofibrillar organization. *FASEB J* *15*,
695 1209-1211.
- 696 9. Hirashima, M., Lu, Y., Byers, L., and Rossant, J. (2003). Trophoblast expression of fms-
697 like tyrosine kinase 1 is not required for the establishment of the maternal-fetal interface
698 in the mouse placenta. *Proceedings of the National Academy of Sciences of the United*
699 *States of America* *100*, 15637-15642. [10.1073/pnas.2635424100](https://doi.org/10.1073/pnas.2635424100).
- 700 10. Achen, M.G., Gad, J.M., Stacker, S.A., and Wilks, A.F. (1997). Placenta growth factor
701 and vascular endothelial growth factor are co-expressed during early embryonic
702 development. *Growth Factors* *15*, 69-80. [10.3109/08977199709002113](https://doi.org/10.3109/08977199709002113).
- 703 11. Tsai, F.Y., Keller, G., Kuo, F.C., Weiss, M., Chen, J., Rosenblatt, M., Alt, F.W., and
704 Orkin, S.H. (1994). An early haematopoietic defect in mice lacking the transcription
705 factor GATA-2. *Nature* *371*, 221-226.
- 706 12. Pandolfi, P.P., Roth, M.E., Karis, A., Leonard, M.W., Dzierzak, E., Grosveld, F.G., Engel,
707 J.D., and Lindenbaum, M.H. (1995). Targeted disruption of the GATA3 gene causes
708 severe abnormalities in the nervous system and in fetal liver haematopoiesis. *Nature*
709 *genetics* *11*, 40-44. [10.1038/ng0995-40](https://doi.org/10.1038/ng0995-40).
- 710 13. Ray, S., Dutta, D., Rumi, M.A.K., Kent, L.N., Soares, M.J., and Paul, S. (2009). Context-
711 dependent function of regulatory elements and a switch in chromatin occupancy
712 between GATA3 and GATA2 regulate Gata2 transcription during trophoblast
713 differentiation. *The Journal of biological chemistry* *284*, 4978-4988.
714 [10.1074/jbc.M807329200](https://doi.org/10.1074/jbc.M807329200).
- 715 14. Home, P., Ray, S., Dutta, D., Bronshteyn, I., Larson, M., and Paul, S. (2009). GATA3 is
716 selectively expressed in the trophectoderm of peri-implantation embryo and directly
717 regulates Cdx2 gene expression. *J Biol Chem* *284*, 28729-28737.
718 [10.1074/jbc.M109.016840](https://doi.org/10.1074/jbc.M109.016840).
- 719 15. Ghosh, A., Kumar, R., Kumar, R.P., Ray, S., Saha, A., Roy, N., Dasgupta, P., Marsh, C.,
720 and Paul, S. (2024). The GATA transcriptional program dictates cell fate equilibrium to

- 721 establish the maternal-fetal exchange interface and fetal development. *Proc Natl Acad*
722 *Sci U S A* *121*, e2310502121. 10.1073/pnas.2310502121.
- 723 16. Ng, Y.K., George, K.M., Engel, J.D., and Linzer, D.I.H. (1994). Gata Factor Activity Is
724 Required for the Trophoblast-Specific Transcriptional Regulation of the Mouse Placental-
725 Lactogen-I Gene. *Development* *120*, 3257-3266.
- 726 17. Ma, G.T., Roth, M.E., Groskopf, J.C., Tsai, F.Y., Orkin, S.H., Grosveld, F., Engel, J.D.,
727 and Linzer, D.I. (1997). GATA-2 and GATA-3 regulate trophoblast-specific gene
728 expression in vivo. *Development (Cambridge, England)* *124*, 907-914.
- 729 18. Jackson, D., Volpert, O.V., Bouck, N., and Linzer, D.I. (1994). Stimulation and inhibition
730 of angiogenesis by placental proliferin and proliferin-related protein. *Science* *266*, 1581-
731 1584. 10.1126/science.7527157.
- 732 19. Home, P., Kumar, R.P., Ganguly, A., Saha, B., Milano-Foster, J., Bhattacharya, B., Ray,
733 S., Gunewardena, S., Paul, A., Camper, S.A., et al. (2017). Genetic redundancy of
734 GATA factors in the extraembryonic trophoblast lineage ensures the progression of
735 preimplantation and postimplantation mammalian development. *Development* *144*, 876-
736 888. 10.1242/dev.145318.
- 737 20. Simmons, D.G., Fortier, A.L., and Cross, J.C. (2007). Diverse subtypes and
738 developmental origins of trophoblast giant cells in the mouse placenta. *Dev Biol* *304*,
739 567-578. 10.1016/j.ydbio.2007.01.009.
- 740 21. Bany, B.M., and Cross, J.C. (2006). Post-implantation mouse conceptuses produce
741 paracrine signals that regulate the uterine endometrium undergoing decidualization. *Dev*
742 *Biol* *294*, 445-456. 10.1016/j.ydbio.2006.03.006.
- 743 22. Ouseph, M.M., Li, J., Chen, H.Z., Pecot, T., Wenzel, P., Thompson, J.C., Comstock, G.,
744 Chokshi, V., Byrne, M., Forde, B., et al. (2012). Atypical E2F repressors and activators
745 coordinate placental development. *Dev Cell* *22*, 849-862. 10.1016/j.devcel.2012.01.013.
- 746 23. Jiang, X., Wang, Y., Xiao, Z., Yan, L., Guo, S., Wang, Y., Wu, H., Zhao, X., Lu, X., and
747 Wang, H. (2023). A differentiation roadmap of murine placentation at single-cell
748 resolution. *Cell Discovery* *9*, 30. 10.1038/s41421-022-00513-z.
- 749 24. Simmons, D.G., and Cross, J.C. (2005). Determinants of trophoblast lineage and cell
750 subtype specification in the mouse placenta. *Developmental biology* *284*, 12-24.
751 10.1016/j.ydbio.2005.05.010.
- 752 25. Muzumdar, M.D., Tasic, B., Miyamichi, K., Li, L., and Luo, L. (2007). A global double-
753 fluorescent Cre reporter mouse. *Genesis* *45*, 593-605. 10.1002/dvg.20335.
- 754 26. Mikkola, H.K., and Orkin, S.H. (2006). The journey of developing hematopoietic stem
755 cells. *Development* *133*, 3733-3744. 10.1242/dev.02568.
- 756 27. El-Hashash, A.H.K., Warburton, D., and Kimber, S.J. (2009). Genes and signals
757 regulating murine trophoblast cell development. *Mechanisms of development* *127*, 1-20.
758 10.1016/j.mod.2009.09.004.
- 759 28. Bany, B.M., and Cross, J.C. (2006). Post-implantation mouse conceptuses produce
760 paracrine signals that regulate the uterine endometrium undergoing decidualization.
761 *Developmental Biology* *294*, 445-456. 10.1016/j.ydbio.2006.03.006.
- 762 29. Carney, E.W., Prideaux, V., Lye, S.J., and Rossant, J. (1993). Progressive expression of
763 trophoblast-specific genes during formation of mouse trophoblast giant cells in vitro. *Mol*
764 *Reprod Dev* *34*, 357-368. 10.1002/mrd.1080340403.
- 765 30. Parisi, T., Beck, A.R., Rougier, N., McNeil, T., Lucian, L., Werb, Z., and Amati, B. (2003).
766 Cyclins E1 and E2 are required for endoreplication in placental trophoblast giant cells.
767 *EMBO J* *22*, 4794-4803. 10.1093/emboj/cdg482.
- 768 31. Han, X., Wang, R., Zhou, Y., Fei, L., Sun, H., Lai, S., Saadatpour, A., Zhou, Z., Chen,
769 H., Ye, F., et al. (2018). Mapping the Mouse Cell Atlas by Microwell-Seq. *Cell* *173*, 1307.
770 10.1016/j.cell.2018.05.012.

- 771 32. Simmons, D.G., Fortier, A.L., and Cross, J.C. (2007). Diverse subtypes and
772 developmental origins of trophoblast giant cells in the mouse placenta. *Developmental*
773 *biology* *304*, 567-578. 10.1016/j.ydbio.2007.01.009.
- 774 33. Natale, B.V., Schweitzer, C., Hughes, M., Globisch, M.A., Kotadia, R., Tremblay, E., Vu,
775 P., Cross, J.C., and Natale, D.R.C. (2017). Sca-1 identifies a trophoblast population with
776 multipotent potential in the mid-gestation mouse placenta. *Sci Rep* *7*, 5575.
777 10.1038/s41598-017-06008-2.
- 778 34. Muntener, M., and Hsu, Y.C. (1977). Development of trophoblast and placenta of the
779 mouse. A reinvestigation with regard to the in vitro culture of mouse trophoblast and
780 placenta. *Acta Anat (Basel)* *98*, 241-252.
- 781 35. Linzer, D.I., and Fisher, S.J. (1999). The placenta and the prolactin family of hormones:
782 regulation of the physiology of pregnancy. *Mol Endocrinol* *13*, 837-840.
783 10.1210/mend.13.6.0286.
- 784 36. Yotsumoto, S., Shimada, T., Cui, C.Y., Nakashima, H., Fujiwara, H., and Ko, M.S.H.
785 (1998). Expression of adrenomedullin, a hypotensive peptide, in the trophoblast giant
786 cells at the embryo implantation site in mouse. *Developmental Biology* *203*, 264-275.
787 DOI 10.1006/dbio.1998.9073.
- 788 37. WeilerGuettler, H., Aird, W.C., Rayburn, H., Husain, M., and Rosenberg, R.D. (1996).
789 Developmentally regulated gene expression of thrombomodulin in postimplantation
790 mouse embryos. *Development* *122*, 2271-2281.
- 791 38. Lee, S.J., Talamantes, F., Wilder, E., Linzer, D.I.H., and Nathans, D. (1988).
792 Trophoblastic Giant-Cells of the Mouse Placenta as the Site of Proliferin Synthesis.
793 *Endocrinology* *122*, 1761-1768. DOI 10.1210/endo-122-5-1761.
- 794 39. Cross, J.C., Hemberger, M., Lu, Y., Nozaki, T., Whiteley, K., Masutani, M., and
795 Adamson, S.L. (2002). Trophoblast functions, angiogenesis and remodeling of the
796 maternal vasculature in the placenta. *Mol Cell Endocrinol* *187*, 207-212.
- 797 40. Gekas, C., Dieterlen-Lievre, F., Orkin, S.H., and Mikkola, H.K.A. (2005). The placenta is
798 a niche for hematopoietic stem cells. *Developmental Cell* *8*, 365-375. DOI
799 10.1016/j.devcel.2004.12.016.
- 800 41. Bollerot, K., Pouget, C., and Jaffredo, T. (2005). The embryonic origins of hematopoietic
801 stem cells: a tale of hemangioblast and hemogenic endothelium. *APMIS* *113*, 790-803.
802 10.1111/j.1600-0463.2005.apm_317.x.
- 803 42. Shalaby, F., Rossant, J., Yamaguchi, T.P., Gertsenstein, M., Wu, X.F., Breitman, M.L.,
804 and Schuh, A.C. (1995). Failure of blood-island formation and vasculogenesis in Flk-1-
805 deficient mice. *Nature* *376*, 62-66. 10.1038/376062a0.
- 806 43. Shalaby, F., Ho, J., Stanford, W.L., Fischer, K.D., Schuh, A.C., Schwartz, L., Bernstein,
807 A., and Rossant, J. (1997). A requirement for Flk1 in primitive and definitive
808 hematopoiesis and vasculogenesis. *Cell* *89*, 981-990. Doi 10.1016/S0092-
809 8674(00)80283-4.
- 810 44. Choi, K., Kennedy, M., Kazarov, A., Papadimitriou, J.C., and Keller, G. (1998). A
811 common precursor for hematopoietic and endothelial cells. *Development* *125*, 725-732.
- 812 45. Kim, I., Yilmaz, O.H., and Morrison, S.J. (2005). CD144 (VE-cadherin) is transiently
813 expressed by fetal liver hematopoietic stem cells. *Blood* *106*, 903-905. 10.1182/blood-
814 2004-12-4960.
- 815 46. Nasrallah, R., Fast, E.M., Solaimani, P., Knezevic, K., Eliades, A., Patel, R.,
816 Thambyrajah, R., Unnikrishnan, A., Thoms, J., Beck, D., et al. (2016). Identification of
817 novel regulators of developmental hematopoiesis using Endoglin regulatory elements as
818 molecular probes. *Blood* *128*, 1928-1939. 10.1182/blood-2016-02-697870.
- 819 47. Kubo, A., Chen, V., Kennedy, M., Zahradka, E., Daley, G.Q., and Keller, G. (2005). The
820 homeobox gene HEX regulates proliferation and differentiation of hemangioblasts and

- endothelial cells during ES cell differentiation. *Blood* *105*, 4590-4597. 10.1182/blood-2004-10-4137.
- 823 48. Park, M.A., Kumar, A., Jung, H.S., Uenishi, G., Moskvina, O.V., Thomson, J.A., and
824 Slukvin, I.I. (2018). Activation of the Arterial Program Drives Development of Definitive
825 Hemogenic Endothelium with Lymphoid Potential. *Cell Rep* *23*, 2467-2481.
826 10.1016/j.celrep.2018.04.092.
- 827 49. Marcelo, K.L., Goldie, L.C., and Hirschi, K.K. (2013). Regulation of endothelial cell
828 differentiation and specification. *Circ Res* *112*, 1272-1287.
829 10.1161/CIRCRESAHA.113.300506.
- 830 50. Pereira, C.F., Chang, B., Gomes, A., Bernitz, J., Papatsenko, D., Niu, X., Swiers, G.,
831 Azzoni, E., de Bruijn, M.F., Schaniel, C., et al. (2016). Hematopoietic Reprogramming In
832 Vitro Informs In Vivo Identification of Hemogenic Precursors to Definitive Hematopoietic
833 Stem Cells. *Dev Cell* *36*, 525-539. 10.1016/j.devcel.2016.02.011.
- 834 51. Azevedo Portilho, N., and Pelajo-Machado, M. (2018). Mechanism of hematopoiesis and
835 vasculogenesis in mouse placenta. *Placenta* *69*, 140-145.
836 10.1016/j.placenta.2018.04.007.
- 837 52. North, T.E., de Bruijn, M.F.T.R., Stacy, T., Talebian, L., Lind, E., Robin, C., Binder, M.,
838 Dzierzak, E., and Speck, N.A. (2002). Runx1 expression marks long-term repopulating
839 hematopoietic stem cells in the midgestation mouse embryo. *Immunity* *16*, 661-672. Doi
840 10.1016/S1074-7613(02)00296-0.
- 841 53. Lee, L.K., Ueno, M., Van Handel, B., and Mikkola, H.K.A. (2010). Placenta as a newly
842 identified source of hematopoietic stem cells. *Curr Opin Hematol* *17*, 313-318.
843 10.1097/MOH.0b013e328339f295.
- 844 54. Mahony, C.B., and Bertrand, J.Y. (2019). How HSCs Colonize and Expand in the Fetal
845 Niche of the Vertebrate Embryo: An Evolutionary Perspective. *Front Cell Dev Biol* *7*.
846 UNSP 34
10.3389/fcell.2019.00034.
- 847 55. Breier, G. (2000). Angiogenesis in embryonic development--a review. *Placenta* *21 Suppl*
848 *A*, S11-15.
- 849 56. Drake, C.J., and Fleming, P.A. (2000). Vasculogenesis in the day 6.5 to 9.5 mouse
850 embryo. *Blood* *95*, 1671-1679.
- 851 57. Carmeliet, P., Moons, L., Luttun, A., Vincenti, V., Compernelle, V., De Mol, M., Wu, Y.,
852 Bono, F., Devy, L., Beck, H., et al. (2001). Synergism between vascular endothelial
853 growth factor and placental growth factor contributes to angiogenesis and plasma
854 extravasation in pathological conditions. *Nat Med* *7*, 575-583. 10.1038/87904.
- 855 58. Palmer, K.R., Tong, S., and Kaitu'u-Lino, T.J. (2017). Placental-specific sFLT-1: role in
856 pre-eclamptic pathophysiology and its translational possibilities for clinical prediction and
857 diagnosis. *Mol Hum Reprod* *23*, 69-78. 10.1093/molehr/gaw077.
- 858 59. Hu, D., and Cross, J.C. (2010). Development and function of trophoblast giant cells in
859 the rodent placenta. *Int J Dev Biol* *54*, 341-354. 10.1387/ijdb.082768dh.
- 860 60. Tyler, S.R., Rotti, P.G., Sun, X., Yi, Y., Xie, W., Winter, M.C., Flamme-Wiese, M.J.,
861 Tucker, B.A., Mullins, R.F., Norris, A.W., and Engelhardt, J.F. (2019). PyMINER Finds
862 Gene and Autocrine-Paracrine Networks from Human Islet scRNA-Seq. *Cell Rep* *26*,
863 1951-1964 e1958. 10.1016/j.celrep.2019.01.063.
- 864 61. Lee, C.Q.E., Turco, M.Y., Gardner, L., Simons, B.D., Hemberger, M., and Moffett, A.
865 (2018). Integrin alpha2 marks a niche of trophoblast progenitor cells in first trimester
866 human placenta. *Development* *145*. 10.1242/dev.162305.
- 867 62. Bader, B.L., Rayburn, H., Crowley, D., and Hynes, R.O. (1998). Extensive
868 vasculogenesis, angiogenesis, and organogenesis precede lethality in mice lacking all
869 alpha v integrins. *Cell* *95*, 507-519. 10.1016/s0092-8674(00)81618-9.
- 870

- 871 63. Welser, J.V., Lange, N.D., Flintoff-Dye, N., Burkin, H.R., and Burkin, D.J. (2007).
872 Placental defects in alpha7 integrin null mice. *Placenta* 28, 1219-1228.
873 10.1016/j.placenta.2007.08.002.
- 874 64. Wiemers, D.O., Shao, L.J., Ain, R., Dai, G., and Soares, M.J. (2003). The mouse
875 prolactin gene family locus. *Endocrinology* 144, 313-325. 10.1210/en.2002-220724.
- 876 65. Simmons, D.G., Rawn, S., Davies, A., Hughes, M., and Cross, J.C. (2008). Spatial and
877 temporal expression of the 23 murine Prolactin/Placental Lactogen-related genes is not
878 associated with their position in the locus. *BMC Genomics* 9, 352. 10.1186/1471-2164-9-
879 352.
- 880 66. Johnson, M.P., Brennecke, S.P., East, C.E., Goring, H.H., Kent, J.W., Jr., Dyer, T.D.,
881 Said, J.M., Roten, L.T., Iversen, A.C., Abraham, L.J., et al. (2012). Genome-wide
882 association scan identifies a risk locus for preeclampsia on 2q14, near the inhibin, beta
883 B gene. *PLoS One* 7, e33666. 10.1371/journal.pone.0033666.
- 884 67. Marsh, B., and Blelloch, R. (2020). Single nuclei RNA-seq of mouse placental labyrinth
885 development. *Elife* 9. 10.7554/eLife.60266.
- 886 68. Okae, H., Toh, H., Sato, T., Hiura, H., Takahashi, S., Shirane, K., Kabayama, Y.,
887 Suyama, M., Sasaki, H., and Arima, T. (2018). Derivation of Human Trophoblast Stem
888 Cells. *Cell Stem Cell* 22, 50-63 e56. 10.1016/j.stem.2017.11.004.
- 889 69. Paul, S., Home, P., Bhattacharya, B., and Ray, S. (2017). GATA factors: Master
890 regulators of gene expression in trophoblast progenitors. *Placenta* 60 Suppl 1, S61-S66.
891 10.1016/j.placenta.2017.05.005.
- 892 70. Pollheimer, J., Vondra, S., Baltayeva, J., Beristain, A.G., and Knofler, M. (2018).
893 Regulation of Placental Extravillous Trophoblasts by the Maternal Uterine Environment.
894 *Front Immunol* 9, 2597. 10.3389/fimmu.2018.02597.
- 895 71. Arutyunyan, A., Roberts, K., Troule, K., Wong, F.C.K., Sheridan, M.A., Kats, I., Garcia-
896 Alonso, L., Velten, B., Hoo, R., Ruiz-Morales, E.R., et al. (2023). Spatial multiomics map
897 of trophoblast development in early pregnancy. *Nature* 616, 143-151. 10.1038/s41586-
898 023-05869-0.
- 899 72. Charles, M.A., Saunders, T.L., Wood, W.M., Owens, K., Parlow, A.F., Camper, S.A.,
900 Ridgway, E.C., and Gordon, D.F. (2006). Pituitary-specific Gata2 knockout: effects on
901 gonadotrope and thyrotrope function. *Mol Endocrinol* 20, 1366-1377. 10.1210/me.2005-
902 0378.
- 903 73. Zhu, J., Min, B., Hu-Li, J., Watson, C.J., Grinberg, A., Wang, Q., Killeen, N., Urban, J.F.,
904 Guo, L., and Paul, W.E. (2004). Conditional deletion of Gata3 shows its essential
905 function in T(H)1-T(H)2 responses. *Nature Immunology* 5, 1157-1165.
- 906 74. Andrews, S. (2010). FastQC: a quality control tool for high throughput sequence data.
907 Available online at: <http://www.bioinformatics.babraham.ac.uk/projects/fastqc>.
- 908 75. Dobin, A., Davis, C.A., Schlesinger, F., Drenkow, J., Zaleski, C., Jha, S., Batut, P.,
909 Chaisson, M., and Gingeras, T.R. (2013). STAR: ultrafast universal RNA-seq aligner.
910 *Bioinformatics* 29, 15-21. 10.1093/bioinformatics/bts635.
- 911 76. Tanaka, S., Kunath, T., Hadjantonakis, A.K., Nagy, A., and Rossant, J. (1998).
912 Promotion of trophoblast stem cell proliferation by FGF4. *Science* 282, 2072-2075.

913

914

915

916

917
918
919
920
921
922
923
924
925
926
927
928
929
930
931
932

933 **Figure legends**

934 **Fig. 1: Trophoblast giant cell-specific GATA deletion leads to embryonic lethality and**
935 **developmental defects.** (A) Mating strategy to identify the Prl3d1 positive parietal giant cell
936 layer. (B) Cryosections of the *mT/mG Pl1^{Cre}* conceptus show exclusive EGFP expression in the
937 parietal TGCs, indicating the specific nature of the *Pl1^{Cre}* expression. (C) Mating strategy to
938 define the importance of GATA factors in the trophoblast giant cells. (D) E12.5 uterine horn
939 harvested from the above mating contains apparent embryonic resorption sites. (E) Isolated
940 conceptuses associated with GATA PI1-KO embryos show severe developmental defects (*)
941 and size differences (*, *) compared to the control (*). (F) Embryos isolated from one of the

942 extremely small conceptuses (*) reveal gross developmental defects and embryonic death
943 accompanied by small and thin placental tissue. Scale bar 2 mm. (G) Comparison between a
944 GATA PI1-KO embryo (*) and non-PI1^{Cre} littermate (*) indicates fetal growth reduction and
945 apparent blood loss, and defective vasculature in both the embryo proper and the placenta.
946 Fetal liver (marked by red arrow) of the GATA PI1-KO embryo also showed reduced
947 hematopoiesis compared to the control. Scale bar 2 mm. (H) GATA PI1-KO placentae shown in
948 G (*) were of significantly smaller weight compared to the controls (*) (Mean±s.e.m., n=21 for
949 the control, n=18 for the KO, **P≤0.01, analyzed by two-tailed Student's t-test). (I) RNAScope
950 labeling of implantation sites using the *Tpbpa* probe marks the spongiotrophoblast layers. Scale
951 bar 1 mm (J) Quantitative comparison of the relative ratio of *Tpbpa*+ junctional zone area and
952 labyrinth area between the control and GATA PI1-KO implantation sites (Mean±s.e.m., n=5 for
953 each samples, ***P≤0.001, analyzed by two-tailed Student's t-test).

954

955 **Fig. 2: Single Cell RNA-Seq analyses of the TGC-specific GATA factor loss show altered**
956 **placental trophoblast subpopulation.** (A) A t-SNE plot of the aggregate of the hierarchical
957 clustering of 2 control and 2 GATA PI1-KO placental samples shows 33 distinct clusters. (B) t-
958 SNE plots of the aggregate samples show major cell types. (C) Individual t-SNE plots of the
959 control (aggregate of two control samples) and the KO (aggregate of two KO samples) samples
960 show differences in the major cell subtypes. (D) Individual clusters representing trophoblast
961 subtypes show major differences between the control and the KO placentae. Cluster 3,
962 identified as dead cells/ unidentified cell type, were excluded. (E) Comparative t-SNE plot of
963 cells marked by the expression (log 2-fold expression > 0, p-value <0.05) of trophoblast lineage
964 markers *Prl3d1*, *Prl2c2*, *Tpbpa*, *Prl3b1*, *Hand1* in the control (green box) vs GATA PI1-KO (red
965 box) placentae. Expression in only the trophoblast cells are represented. (F) Quantitative
966 analyses of the relative cell percentages for the *Prl3d1*, *Prl2c2*, *Tpbpa*, *Prl3b1*, *Hand1*, *Ly6a*,

967 *and Epcam^{Hi}* positive cells. For all markers except *Epcam^{Hi}*, log 2-fold expression > 0; for
968 *Epcam^{Hi}* log 2-fold expression > 3. All cell numbers were normalized using total trophoblast cell
969 numbers corresponding to the sample. (Mean±s.e.m., n=2 for each sample type, ****P≤0.0001,
970 analyzed by two-tailed Student's t-test).

971

972 **Fig. 3. TGC-specific GATA factor function is essential for the differentiation of the**

973 **hematoendothelial niche.** (A) Comparative t-SNE plots representing the hematopoietic
974 (orange) and endothelial (purple) cell populations in control vs. GATA PI1-KO placentae are
975 shown. Further cluster distribution of these two populations are shown with the orange box
976 (hematopoietic cells) and the purple box (endothelial cells). These subclusters are described in
977 Fig. 2. (B, C) scRNA-seq analyses show cluster 15 and 17 to harbor the *Kit⁺ Cd34⁺ Ly6A⁺*
978 population of HSCs. The t-SNE plots show a marked reduction in the overall cell numbers in
979 cluster 17 and huge increase in the cluster 15 of the GATA PI1-KO placentae compared to the
980 control (Mean±s.e.m., n=2 for each sample type, **P≤0.01, analyzed by unpaired Student's t-
981 test, Two-stage step-up (Benjamini, Krieger, and Yekutieli)). (D) Quantification of the HSC
982 population in cluster 17 of the control vs. GATA PI1-KO placentae. The total number of cells in
983 each sample type were used to calculate the percentage ((Mean±s.e.m., n=2 for each sample
984 type). (E) Endothelial marker *Kdr* is highly expressed in cluster 15, unlike cluster 17, indicating
985 hematoendothelial nature of the cells belonging to cluster 15. This cluster also harbors cells
986 positive for Arterial-specific marker *Dll4* and placental hemogenic endothelium marker *Prom1*.
987 (F) Flow cytometry analyses of Lin⁻ CD45⁻ CD34⁺ KDR⁺ cells show significant increase in the
988 absence of pTGC-specific GATA factors. (G) Box plot of the flow analysis in the panel F. The
989 percentages were calculated against total number of viable cells per sample (Mean±s.e.m., n=19
990 for the control and n=18 for the GATA PI1-KO, **P≤0.01, analyzed by two-tailed Student's t-
991 test).

992

993 **Fig. 4: GATA factor loss in the TGCs results in the loss of the hematopoietic progenitor**
994 **population.** (A) Flow analysis data shows a significant reduction in the HSC population in the
995 knockout placenta. E12.5 placental samples from GATA PI1-KO and control littermate placentae
996 were subjected to flow analysis. Samples were gated for viable cells, followed by gating for
997 single cells. This was followed by selecting cells negative for lineage markers (Lin⁻) and
998 subjecting them to CD45 negative selection. The Lin⁻ CD45⁻ population were further gated for
999 CD34⁺ and Ly6A/E⁺ fraction. Finally these Lin⁻ CD45⁻ CD34⁺ Ly6A/E⁺ cells were gated for KIT⁺
1000 population. The sample gating schematics are depicted using cell numbers representative of the
1001 respective panels. Black arrows show the flow of the steps. (B) Quantitation of the Lin⁻ CD45⁻
1002 CD34⁺ KIT⁺ Ly6A/E⁺ population reveals significant loss of the HSC population in the KO sample.
1003 The counts are normalized against the number of viable cells and are presented as percentages
1004 (Mean±s.e.m., n=26 for the control and n=24 for the KO, **P≤0.01, analyzed by two-tailed
1005 Student's t-test). (C) Micrographs show the formation of hematopoietic cell colonies on a
1006 methylcellulose plate. Colonies included were of CFU-G/M, BFU-E, and CFU-GEMM in nature.
1007 (D) Quantitation of the number of colonies in the control vs. GATA PI1-KO samples. The counts
1008 are normalized against the number of cells plated for each sample (10,000 cells) (Mean±s.e.m.,
1009 n=7 for each sample type, *P<0.05, analyzed by two-tailed Student's t-test).

1010

1011 **Fig. 5: GATA factor-functions in the trophoblast giant cells are essential for the**
1012 **vasculature development at the maternal-fetal interface.** (A-B) Immunostaining of the control
1013 and GATA PI1-KO placenta with the endothelial cell marker CD31 shows abnormal vasculature
1014 development in the GATA PI1-KO in the TGC layer (Scale Bar 200µm). (C) Violin plot shows
1015 *Flt1* expression increases in the GATA PI1-KO placentae compared to the control. The plot
1016 (*log*₂ expression) and the values are derived from the scRNA-seq data and calculated using
1017 Loupe Browser (v 4.1.0) (10x Genomics). For the control, mean=1.63, median=1; for the KO
1018 mean=2.16, median=1.58. n=2 for both sample types. (D) t-SNE plots for *Flt1* expression

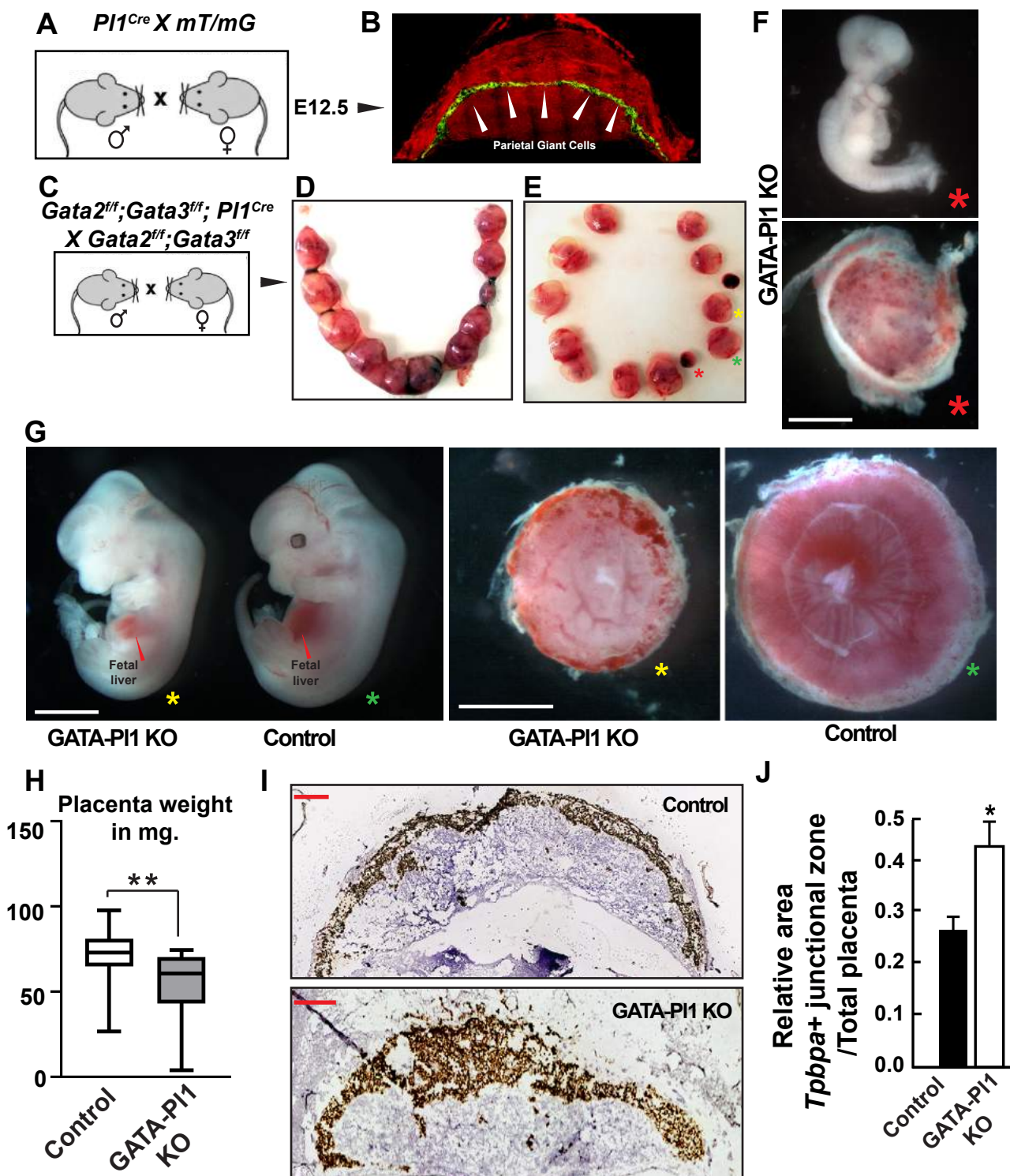
1019 across the clusters show marked increase in the number of *Flt1* expressing cells in the GATA
1020 PI1-KO placentae than control. Some of the major source of *Flt1* expression appears to be the
1021 TGC cluster 33, spiral artery associated TGC cluster 26, hematoendothelial cluster 15 and
1022 spongiotrophoblast trophoblast clusters. (E) Heatmap of cluster-specific *Flt1* expression shows
1023 that the largest change in the *Flt1* expression occurs in the TGC cluster 33 (n=2 for each
1024 sample type). (F) In the presence of conditioned medium from GATA2/GATA3 double knockout
1025 (GATA DKO) trophoblast stem cells, HUMECs fail to form vascular ring-like structures in a
1026 matrigel based vascular tube formation assays unlike when treated with conditioned medium
1027 from control trophoblast stem cells (n=3, Scale Bar 200 μ m).

1028

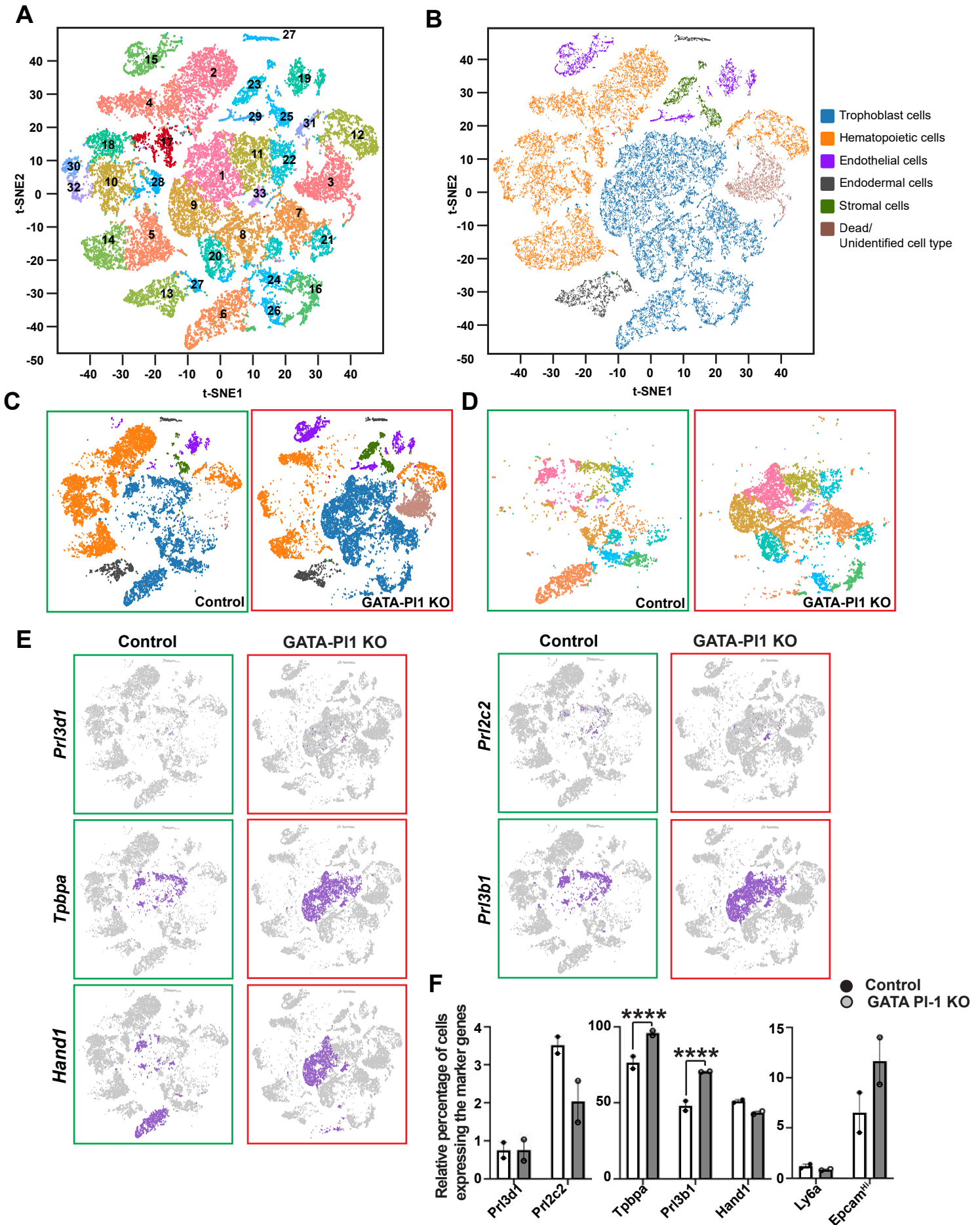
1029 **Fig. 6: The GATA factors regulate parietal TGC-specific paracrine factors and help**
1030 **maintain hematopoietic-angiogenic balance.** (A) PyMINER based prediction of the enriched
1031 paracrine ligands expressed by cells in cluster 33 shows receptor matched targets in four major
1032 clusters that include HSPC/ HSC containing cluster 33, hematoendothelial cluster 15,
1033 trophoblast progenitor cluster 6 and labyrinthine trophoblast cluster 16. Major signaling
1034 pathways involved Integrin signaling pathway members lamin and collagen group 4 of proteins
1035 and prolactin family of hormones. (B) *Prl3d1* expressing cells in cluster 33 were further analyzed
1036 for the level of paracrine factors expression. While almost all the Integrin pathway members
1037 were upregulated, all the prolactin family members showed downregulation in the GATA PI1-KO
1038 samples compared to the control. Average log₂ fold change expression values are plotted. (C)
1039 Immunostaining of E13.5 placental sections with LAMBI and LAMB2 antibodies show increased
1040 expression for both the proteins in the pTGCs of the KO samples than controls (Scale Bar
1041 100 μ m).

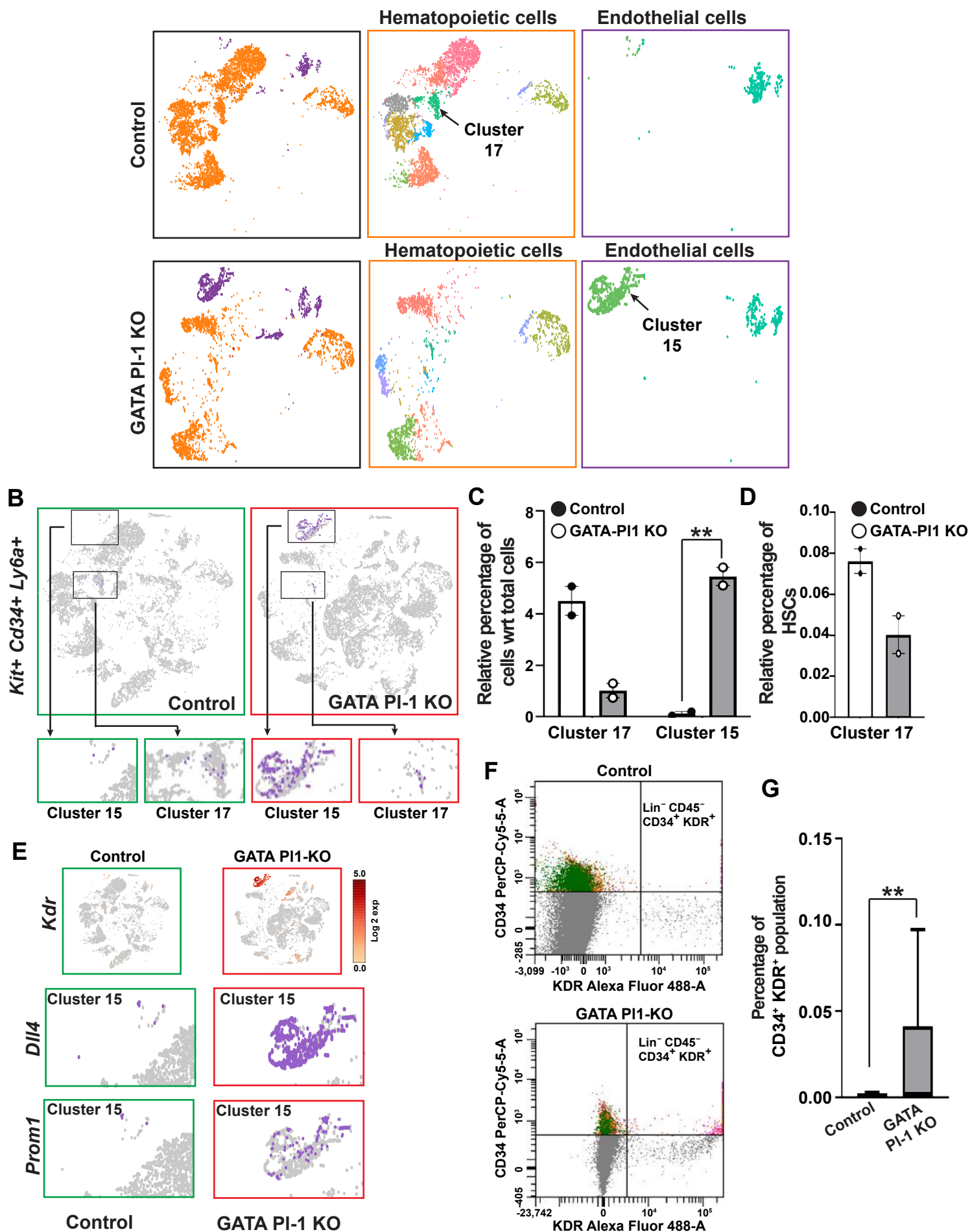
1042

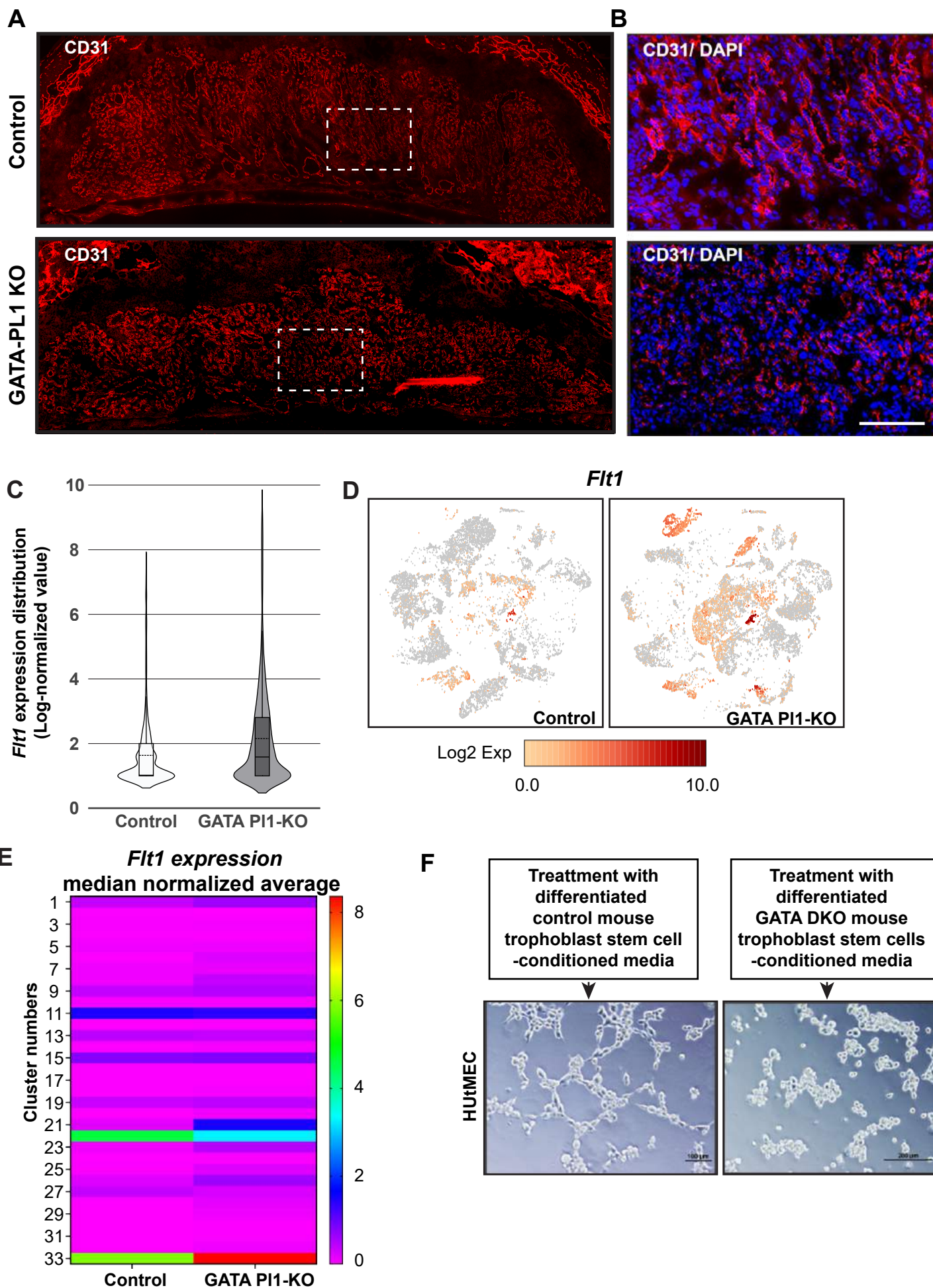
1043 **Fig. 7: TGC-specific Integrin signaling and Prolactin signaling govern placental**
1044 **hematoendothelial differentiation and placental development.** Schematic representation
1045 mid-gestation mouse placenta shows GATA factors regulate parietal-TGC-specific Integrin and
1046 Prolactin signaling. Repression of Integrin signaling and activation of Prolactin signaling by the
1047 GATA factors are achieved in the TGCs, which in turn helps angiogenic development, HSC
1048 development, and proper trophoblast differentiation in a control mouse placenta. In the absence
1049 of the GATA factors, an increase in the Integrin signaling and repression of the Prolactin
1050 signaling trigger loss of angiogenic branching and HSC population. This is accompanied by
1051 abnormal trophoblast differentiation and trophoblast subtype distribution.



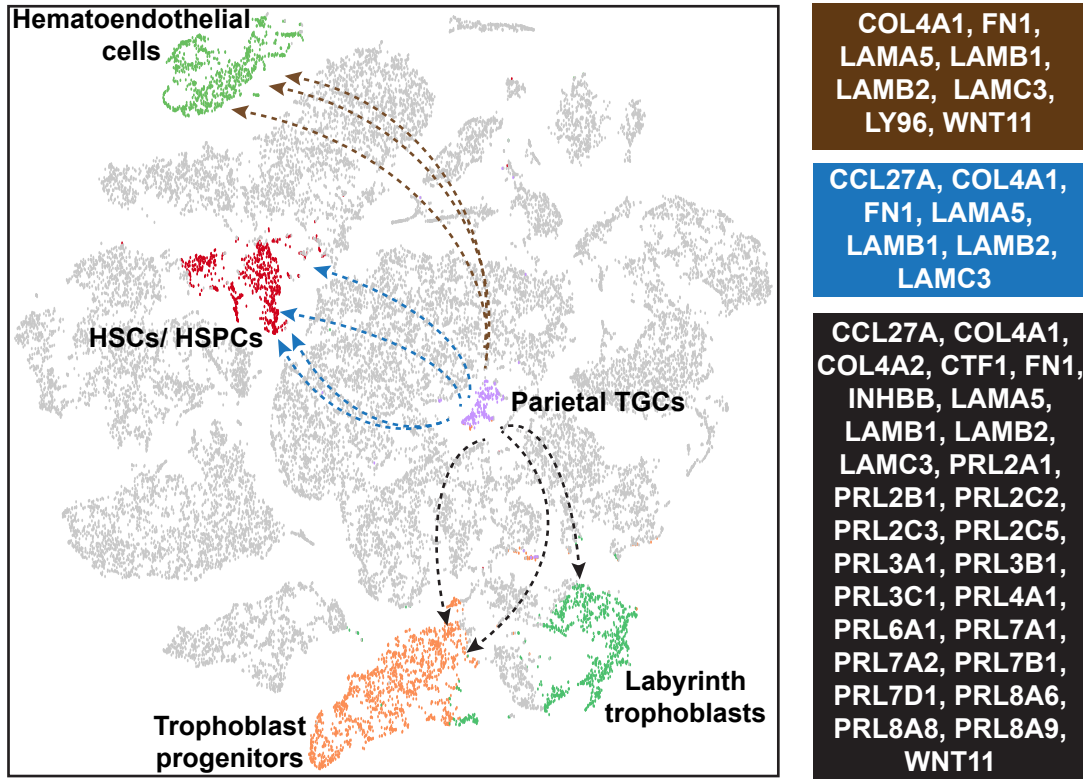
Home_Fig. 2



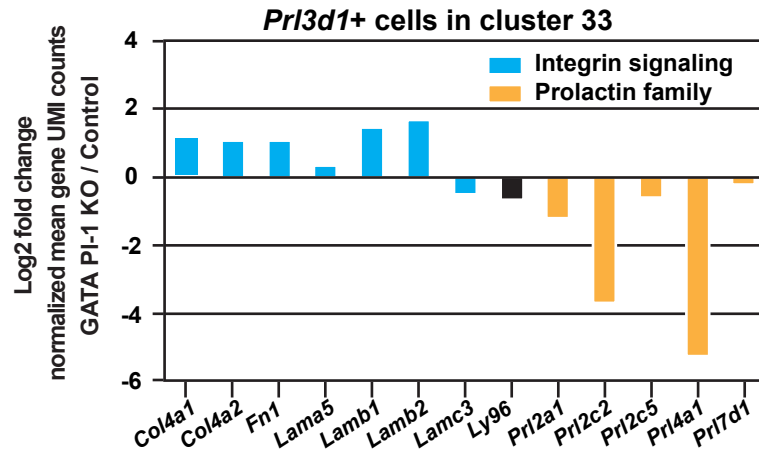




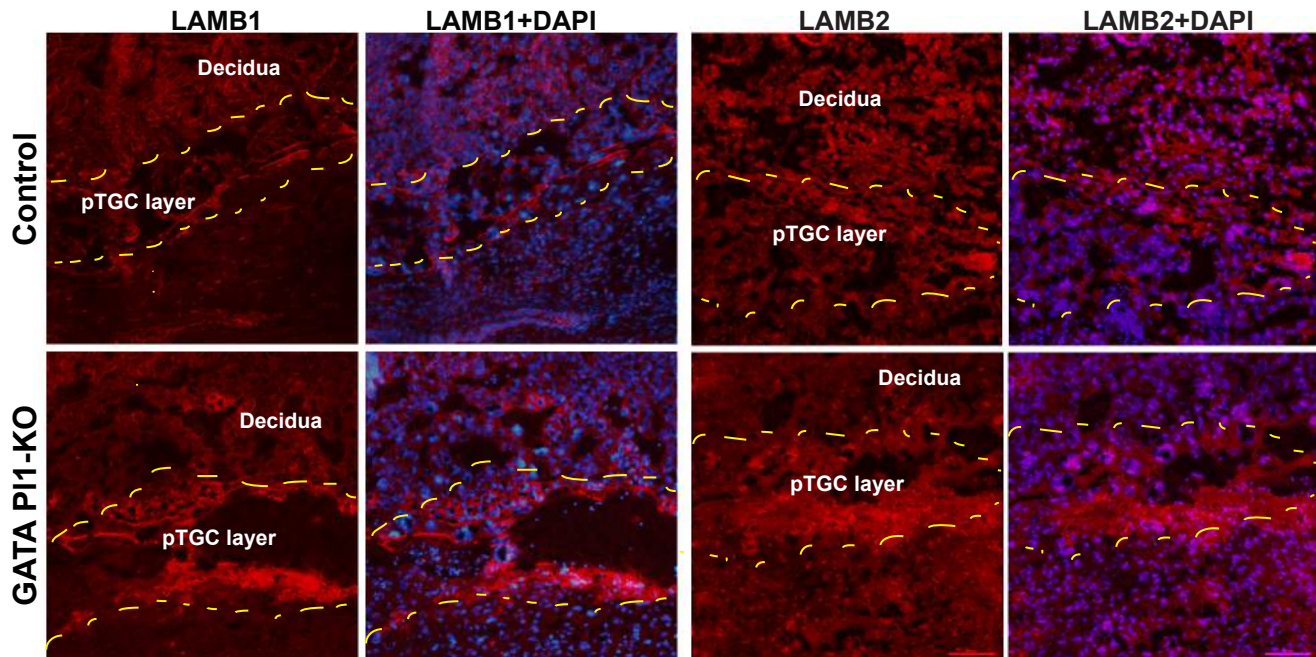
A

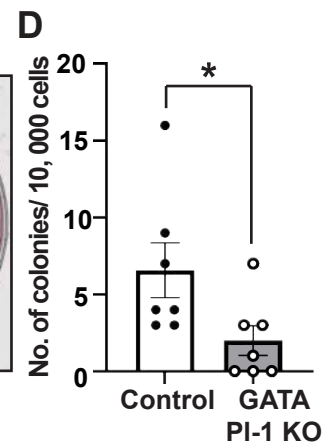
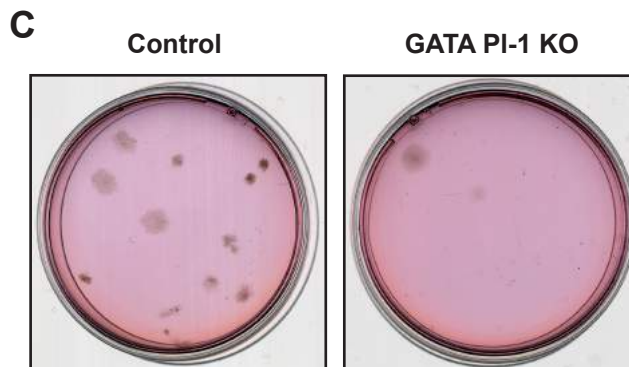
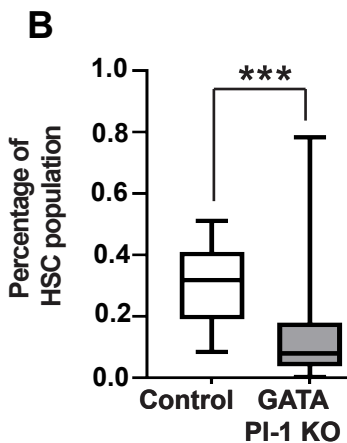
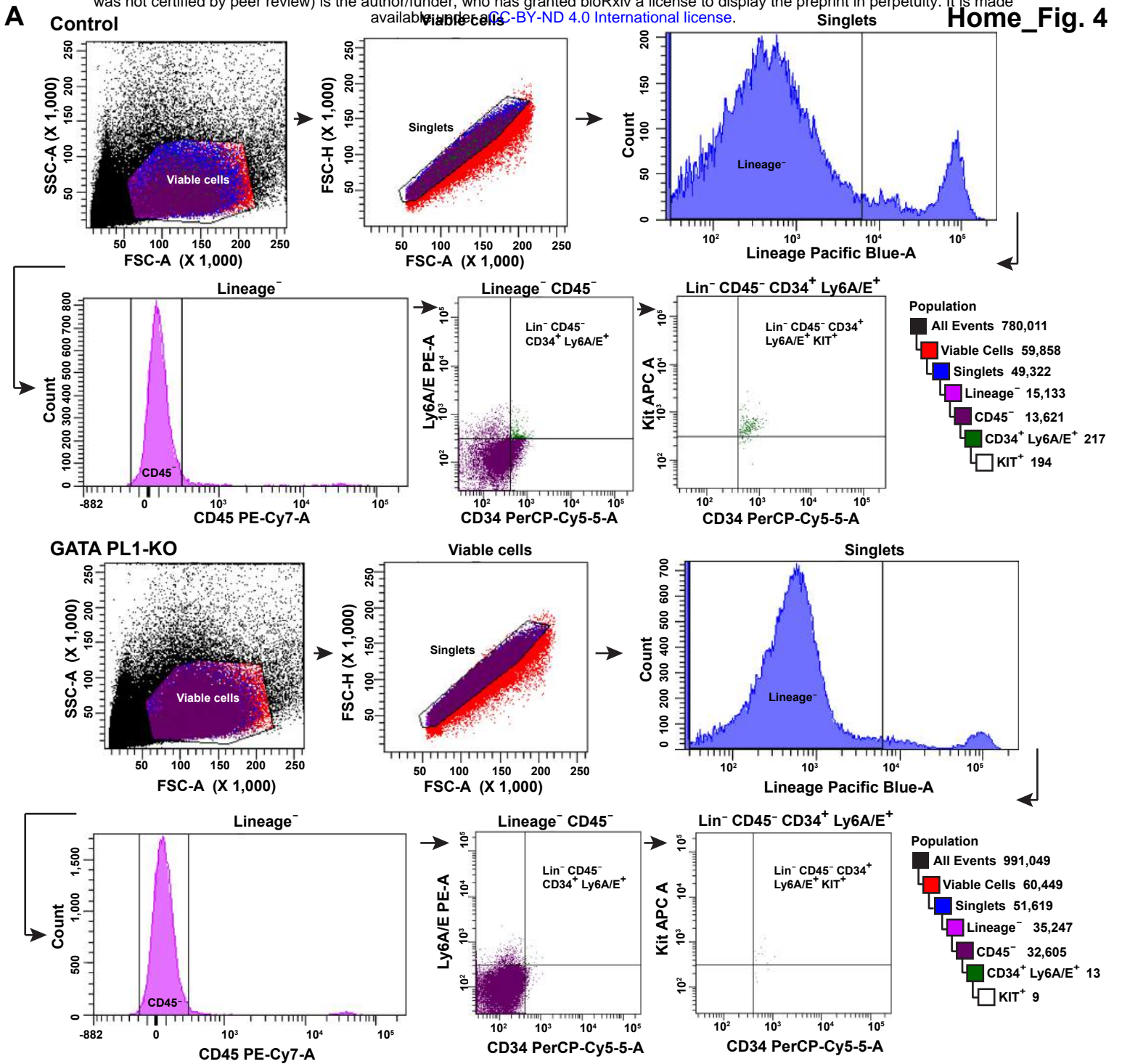


B



C





Home_Fig. 7

